SOLAR ORBITER

RPW Operations Centre

RPW Antenna 3 Nov. 13, 2023, Operation Anomaly Report

ROC-OPS-NMP-RPT-00158-LES
Iss.01, Rev.00

Prepared by:	**Function:**	**Signature:**	**Date**
RPW Team		Signature numérique de Xavier Bonnin Date : 2024.04.23 11:18:57 +02'00'	23/04/2024
Verified by:	**Function:**	**Signature:**	**Date**
RPW Team			Dd/mm/yyyy
Approved by:	**Function:**	**Signature:**	**Date**
Milan Maksimovic	RPW Principal Investigator		Dd/mm/yyyy
For application:	**Function:**	**Signature:**	**Date**
Desi Raulin	Solar Orbiter CNES Project Manager		Dd/mm/yyyy

CLASSIFICATION **PUBLIC** ☒ **RESTRICTED** ☐

l'Observatoire de Paris LESIA
Laboratoire d'Études Spatiales et d'Instrumentation en Astrophysique

CNRS-Observatoire de PARIS
Section de MEUDON – LESIA
5, place Jules Janssen
92195 Meudon Cedex – France

Change Record

Issue	Rev.	Date	Authors	Modifications
1	0	23/04/2024	X.Bonnin and RPW team	First issue

Acronym List

Acronym	Definition
ANT	(Electrical) antennas
AOR	Anomaly Operation Report
ARB	Anomaly Review Board
CNES	Centre National d'Etudes Spatiales
CoI	Co Investigator
CP	Cruise Phase
DPU	Digital Processing Unit
ESA	European Space Agency
ESAC	European Space Astronomy Centre
ESOC	European Space Operation Centre
HF	High Frequency
HFR	High Frequency Receiver
HK	Housekeeping parameters
IOR	Instrument Operation Request
IT	Instrument Team
LF	Low Frequency
LFR	Low Frequence Receiver
LVPS-PDU	Low Voltage Power Supply - Power Distribution Unit
MOC	Solar Orbiter Mission Operation Centre
NECP	Near Earth Commissioning Phase
NMP	Nominal Mission Phase
PA	Preamplifier
PCB	Printed Circuit Board
PDOR	Payload Direct Operation Request
PI	Principal Investigator
ROC	RPW Operation Centre
RPW	Radio and Plasma Waves
RSW	Remote-sensing Window
S/C	Spacecraft
SBM	Selective Burst Mode
SCM	Search Coil Magnetometer
SOAR	Solar Orbiter Archive
SOC	Solar Obriter Science Operation Centre
TC	Telecommand
TDS	Time Domain Sampler
TM	Telemetry
TNR	Thermal Noise Receiver

Table of Contents

List of tables

List of figures

1 GENERAL

1.1 Scope of the Document

This document presents the operation report concerning the RPW electrical antenna 3 (ANT3) anomaly, first observed on-board on November 13, 2023 around 23:36z.

Anomaly activities are tracked in the issue https://gitlab.obspm.fr/ROC/OpsLib/-/issues/250.

1.2 Applicable Documents

This document responds to the requirements of the documents listed in the following table:

Mark	Reference/Iss/Rev	Title of the document	Authors	Date
AD1				
AD2				
AD3				

1.3 Reference Documents

This document is based on the documents listed in the following table:

Mark	Reference/Iss/Rev	Title of the document	Authors	Date
RD1	SOLO-RPWSY-TN-1160-CNES/2/0	RPW instrument user manual	RPW team	18/05/2018
RD2	SOLO-RPW-RP-2490-CNES/1/0	RPW Commissioning activity report	RPW team	21/01/2021
RD3	https://confluence-lesia.obspm.fr/display/ROC/%282024-04-03%29+RPW+ANT3+anomaly	RPW ANT3 anomaly meeting	X.Bonnin	03/04/2024
RD4				

2 OVERVIEW

On November 13, 2023 around 23:36z, RPW temporarily lost its capability to measure signals with the antenna 3 (MY). This problem persisted until Feb 27 at 22:40z when the signal was recovered again. Since then the ANT3 signal has temporarily been lost on a few more occasions (see more information in appendix 0).

The anomaly was first reported by the Bias team, which notified RPW Operation Center (ROC) about an unexpected behavior of the voltage measured on the antenna 3 during the Bias sweep activity performed on-board.

TDS, LFR and TNR-HFR analyzers teams had also confirmed unexpected measurements from antenna 3.

3 DETAILS OF THE ANOMALY

3.1 Operational context

The anomaly occurred during a daily Bias sweep in the STP cycle 283 on November 13, 2023 at ~23:36z. At this time, the instrument activity on-board was nominal and only routine operations were run.

Around the anomaly time, no event was reported by RPW or other payload equipement on-board, but a spacecraft (S/C) disturbance attitude event (“SLEW”) was performed.

Tables in appendices 7.1 and 7.2 give respectively more details about the Solar Orbiter E-FECS and RPW operations planning centred around the incident.

3.2 Results of data analysis

This section gives the results of the anomaly data analysis at this stage of the investigation.

3.2.1 Bias unit

The lost of ANT3 is clearly seen on Figure 1, which shows intensity current I in uA as a function of the potential value V in Volts from Bias sweeps run on-board between ~23:33z and ~23:37z on Nov. 13, 2023 (left plot) and Nov. 14, 2023 (right plot) respectively. While the behavior of signals from ANT1 (black curve) and ANT2 (blue curve) looks as expected on the left plot, the ANT3 data (red curve) becomes noisy when the potential V tends to -60V, then brutally relaxes to 0V at lower intensity current values (i.e., below -25 uA). As seen in the right plot, the sweep realized the next day presents a constant ~0.7V value for ANT3 signal.

Figure 2 presents the potential value V in Volts measured by LFR on the ANT3 (red curve) between 23:36:20z and 23:36:24z during the daily Bias sweep on Nov. 13, 2023. The intensity current I in uA injected in the antenna is plotted in blue dotted. An unexpected event between 23:36:21z and 23:36:22z leads the ANT3 potential V3 to brutally relax to ~0.7V.

Figure 3 shows an example of time series acquired during a Bias calibration performed on-board after the anomaly (here on Dec. 6, 2023). Left plot presents the intensity current I in uA (top) and the LFR potential V in Volts (bottom) as a function of time, measured from the three channels 1 (black), 2 (blue) and 3 (red). Right plot gives the resulting “I versus V” curves for the three channels from the same Bias calibration activity. During Bias calibrations, no anomaly is observed and the data are nominal.

Any problem with the bias electronics is pretty much ruled out: everything works nominally when the calibration relay is flipped, that relay is the only component between the antenna and the parts that work perfectly, and a relay issue can hardly cause a short. This leads to exclude the Bias electronics as a possible origin of the anomaly.

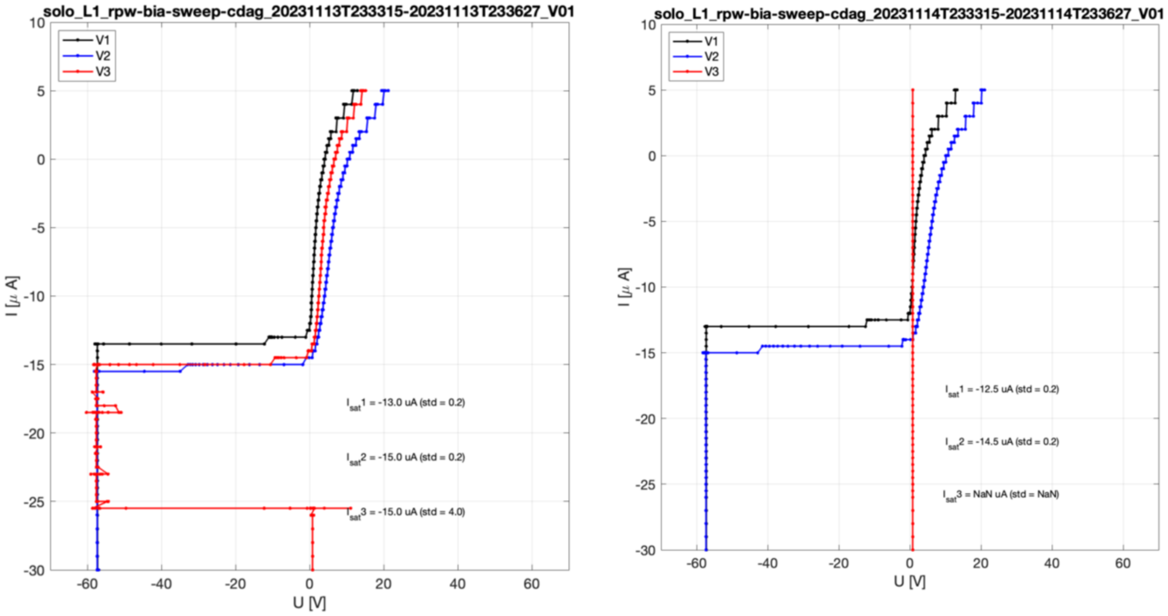

Figure 1. Bias sweeps on Nov. 13, 2023 around 23:33z (left plot). Bias sweeps on Nov. 14, 2023 at the same time (right plot). On Nov. 13 plot, voltage measured on antenna 3 (red curve) promptly tends to ~0.7V after few minutes, which is not expected. Sweeps on the next day (and the followings) show always a ~0.7V vertical line for voltage measured on the antenna 3.

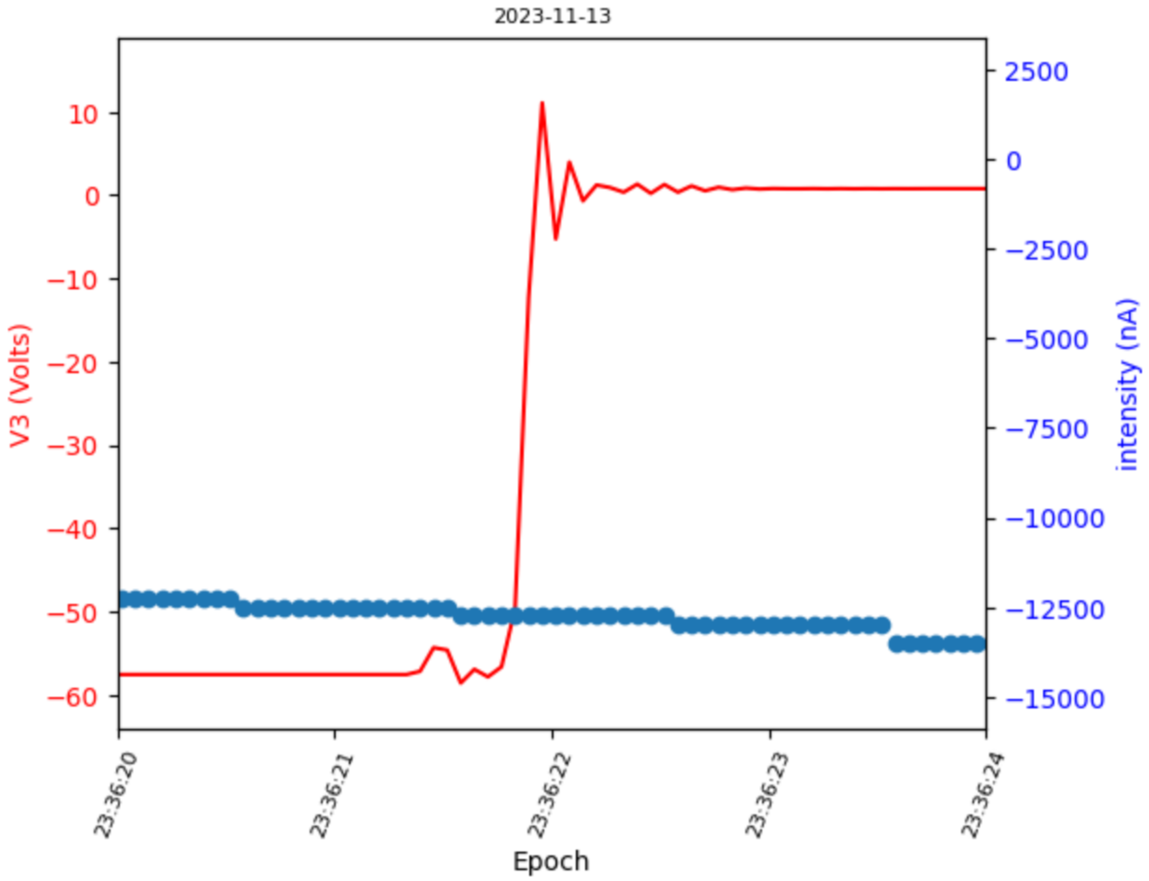

Figure 2. Potential value in Volts measured by LFR on the ANT3 (red curve) between 23:36:20z and 23:36:24z on Nov. 13, 2023. The measurements are acquired during a bias sweep; the intensity current injected in the antenna is plotted here in blue dotted. ANT3 potential brutally returns to 0V between 23:36:21z and 23:36:22z.

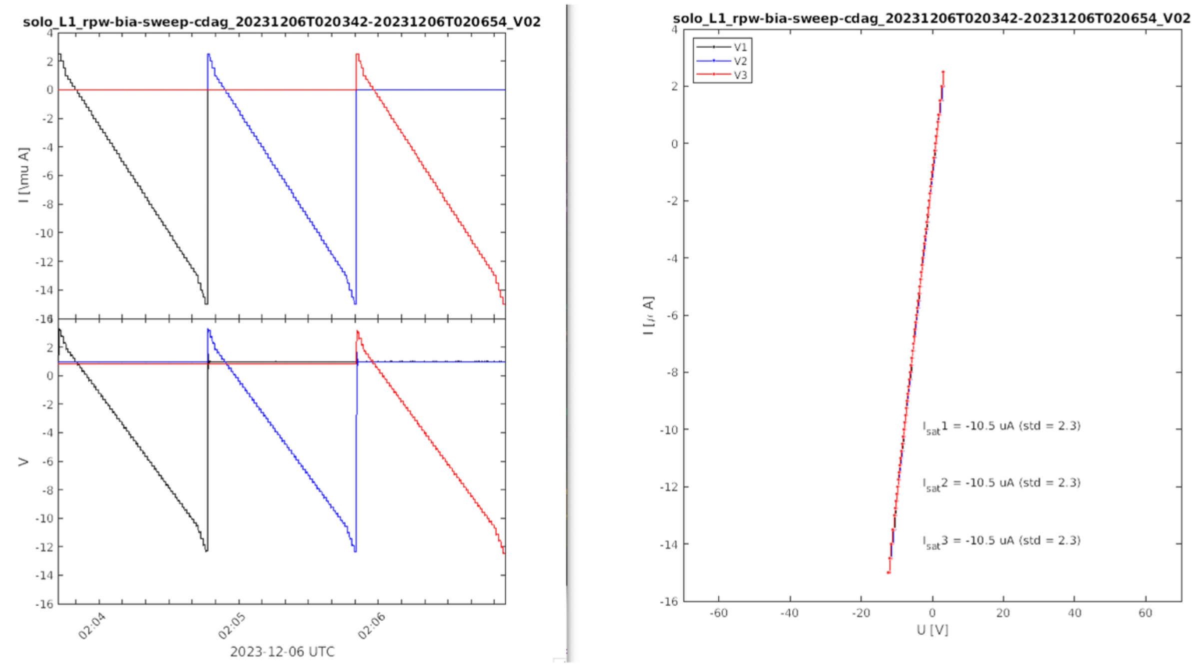

Figure 3. On the left, time series of current intensities (top) in uA and corresponding measured LFR potential in Volts obtained during three successive Bias sweeps performed on each channel 1 (black curve), 2 (blue curve) and 3 (red curve). These bias sweeps were performed on Dec. 06, 2023 (after the incident) during an on-board calibration, when the three Bias channels are connected to the resistors and not to the three antennas. We see from plot on the right (current as a function of voltage) that three channels' curves are perfectly aligned as expected. This indicates that the problem might not come from the Bias electronics.

3.2.2 TDS

At the time of the anomaly, on November 13, 2023, the TDS receiver was in a dipole configuration, sampling voltage differences between atennas V1-V3 and V2-V1. Figure 4 shows the E-field spectrum change at the time of anomaly, clearly demonstrating an increase in the intensity of interference lines on the V1-V3 channel (as the dipole effectively becomes a monopole).

After the anomaly was detected, TDS has been re-configured to sample each antenna V1, V2 and V3 independently in a monopole configuration. The data taken after this change are shown in Figure 5 (spectrogram) and Figure 6 (waveform snapshot). The data clearly show that there is no signal on atenna V3, not even the usual interference lines from the PCDU at around 120 kHz.

The status was unchanged until February 29th , when signal suddenly appeared again in this channel and the antenna seemed to operate normally and provide good data. Since then, however, we have observed several occurrences of a temporary re-occurrence of the anomaly – on March 3, March 9, 10, 11. Except for March 3, the anomaly usuall re-appears a after a BIAS sweep performed around mignight and persists for several hours.

An example of the intermittent re-occurrence from March 3 is show in Figure 7. On this we observe that the signal disappears around 4:00, then briefly re-appears around 11:00 and disappears again. There are several intervals where we observe a "partial" anomaly, with the signal being attenuated, but not completely absent. Figure 8 shows a detailed spectrum corresponding to this partial anomaly. Interrestingly, in this case the low frequency signal disappears while AC signals above ~20 kHz are still observed with some attenuation. This situation could correspond to a capacitive coupling between the preamplifier input and the antenna.

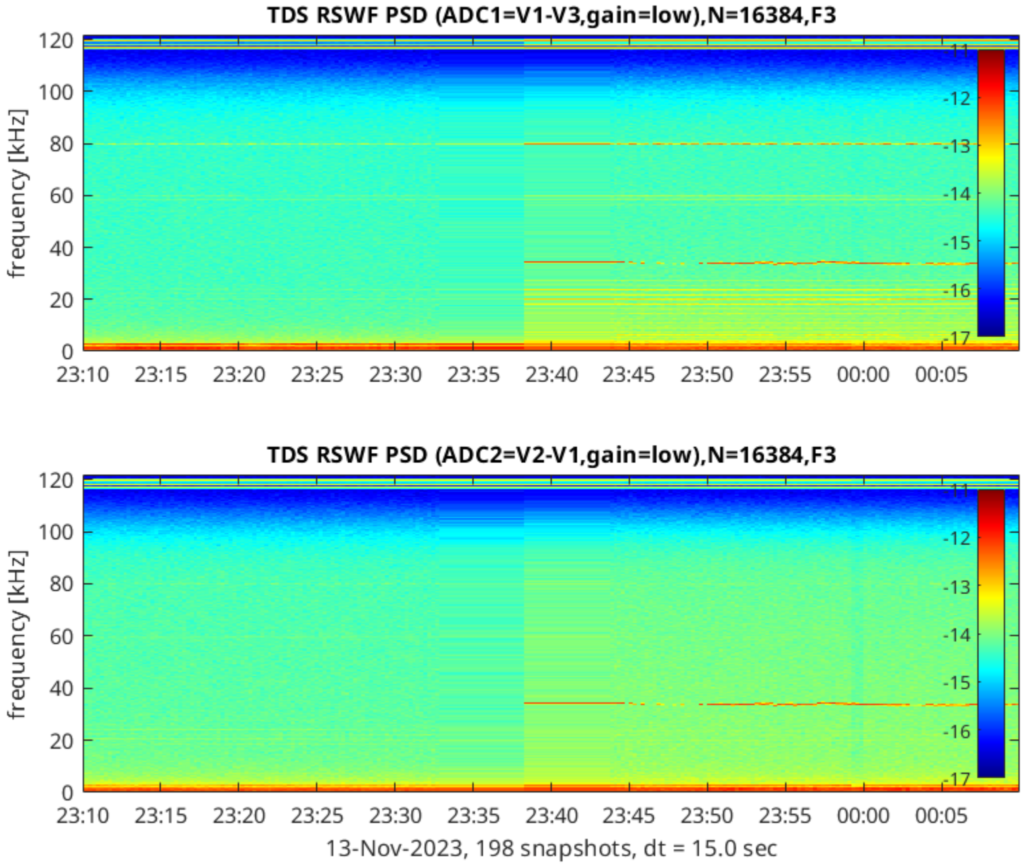

Figure 4. TDS E-field spectrogram around the time of the anomaly.

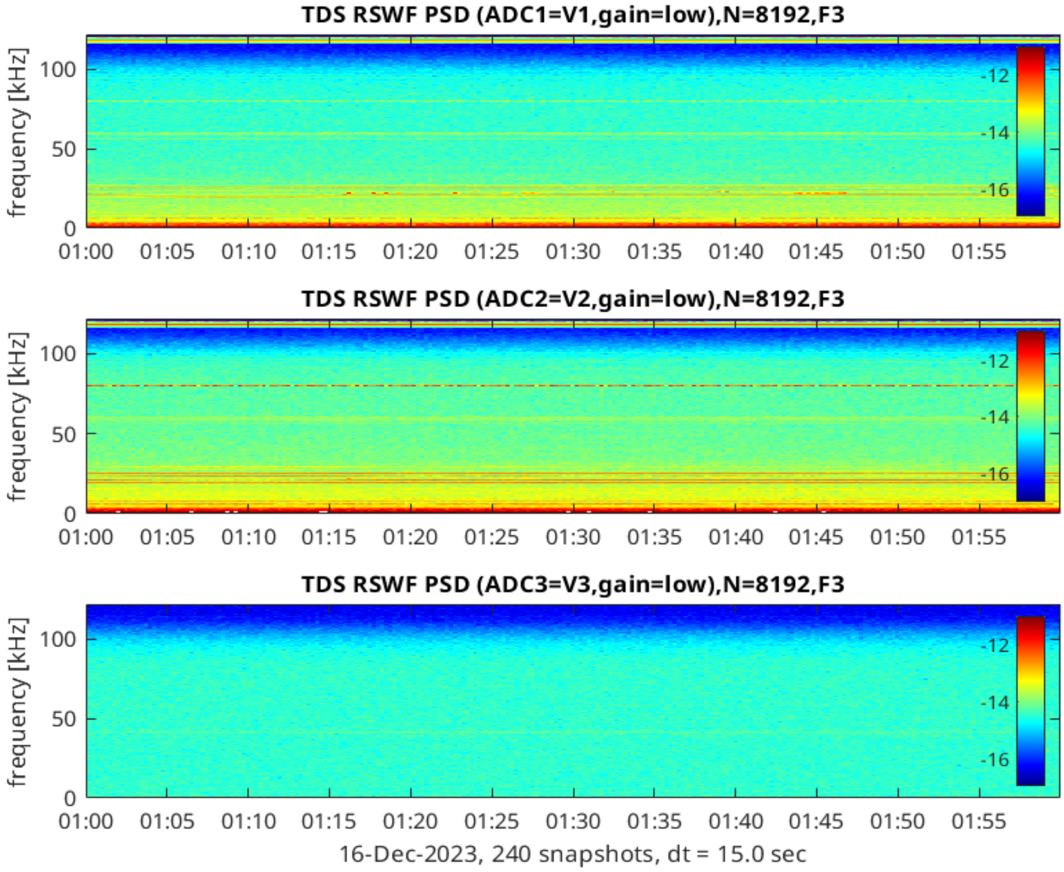

Figure 5. TDS regular snapshot spectrogram after the anomaly, after switching to a monopole antenna configuration.

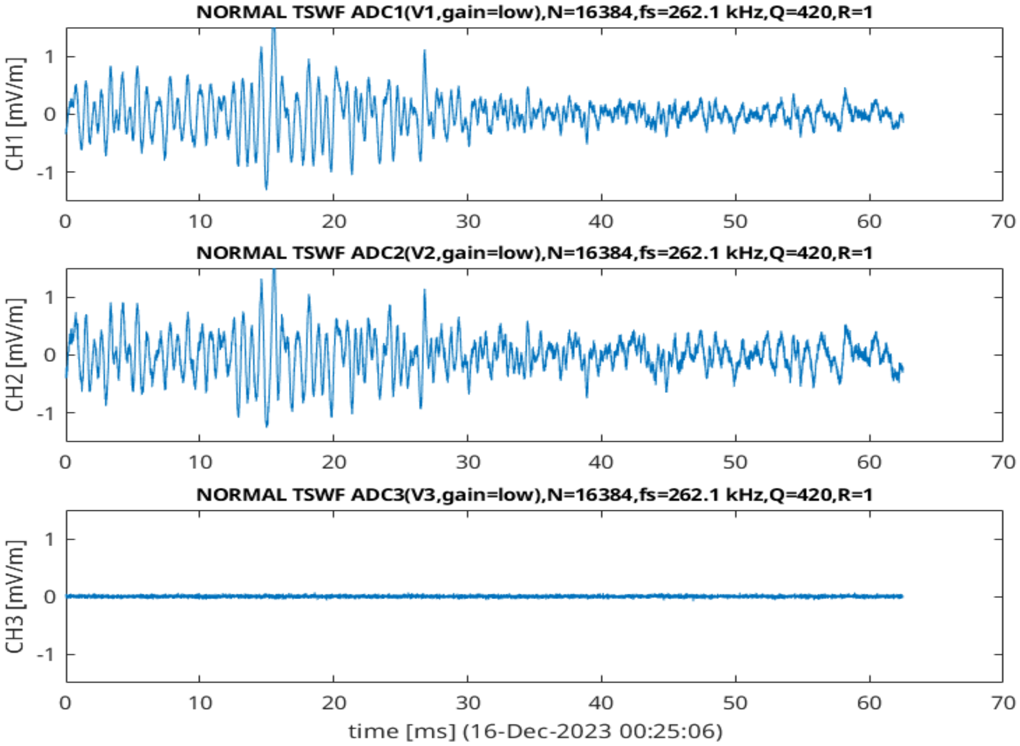

Figure 6. Example of a waveform snapshot from Dec 16, in monopole configuraiton.

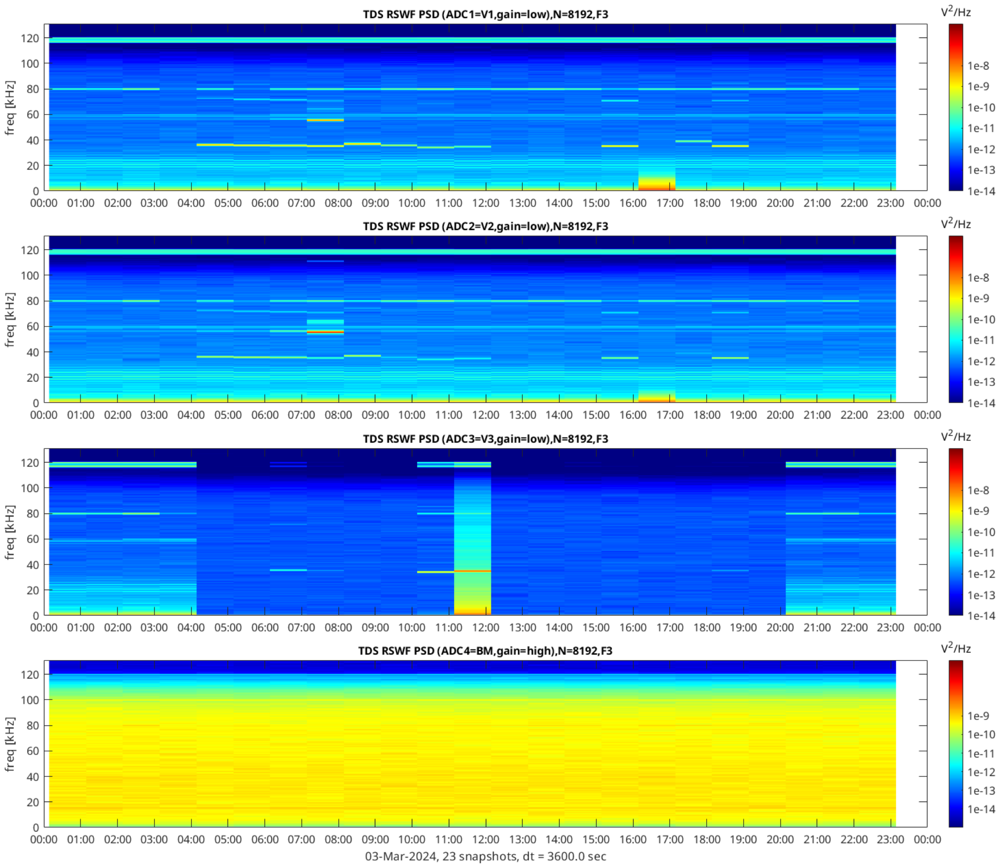

Figure 7. An intermittent re-ocurrence of the anomaly on March 3rd (Regular snapshot spectrum).

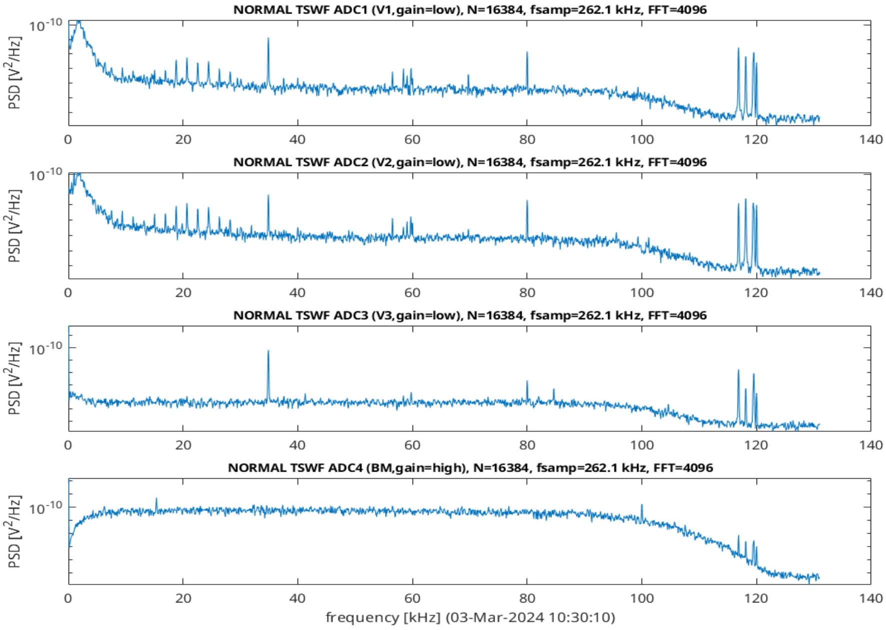

Figure 8. An examples of a detailed spectrum during the intermittent anomaly reocurrence – there V3 antenna shows a « partial » short/disconnect.

3.2.3 LFR

No data analysis was carried out, as the anomaly is not easily visible on LFR spectral products, although it clearly impacts their quality.

3.2.4 THR

3.2.4.1 First diagnosis

On November 13, 2023, around 11:30 p.m., an anomaly occurred on RPW antenna #3. This is manifested by the following observations:

- The loss of the signal on antenna #3, or at least a very strong attenuation of it
- The appearance of interference around 30 kHz

The following figure illustrates this observation from TNR data:

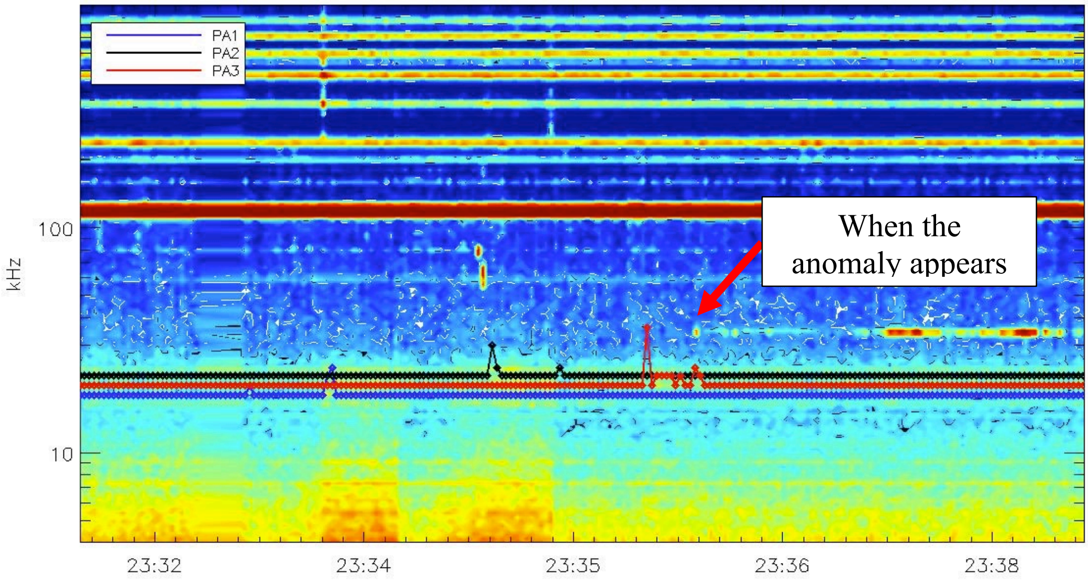

When the anomaly appears

Figure 9. Dynamical spectrum acquired by TNR in V1-V2 dipole on Nov. 13, 2023 around 23:30z. The current HK -5V values of the three PA HF 1, 2 and 3 over time are overploted around 15 kHz.

Note: As on the TDS spectra, we see the appearance of interference around 30 kHz after the breakdown, but we do not perceive an increase in the background on V1-V2.
Everything suggests that, for one reason or another, antenna #3 is short-circuited with the body of the satellite after the occurrence of the anomaly.

3.2.4.2 Diagnostics on the consumption of HF preamps

A check of the consumption of the 3 HF preamps was done via their current HK on voltages +/-5V. The IDs of the concerned HKs are:

- ANT1 PA, +5V : TF_PA_PDU_0027
- ANT1 PA, -5V : TF_PA_PDU_0028
- ANT2 PA, +5V : TF_PA_PDU_0029
- ANT2 PA, -5V : TF_PA_PDU_0030
- ANT3 PA, +5V : TF_PA_PDU_0031

- ANT3 PA, -5V : TF_PA_PDU_0032

The currents absorbed at the time of the breakdown are represented in the following figures:

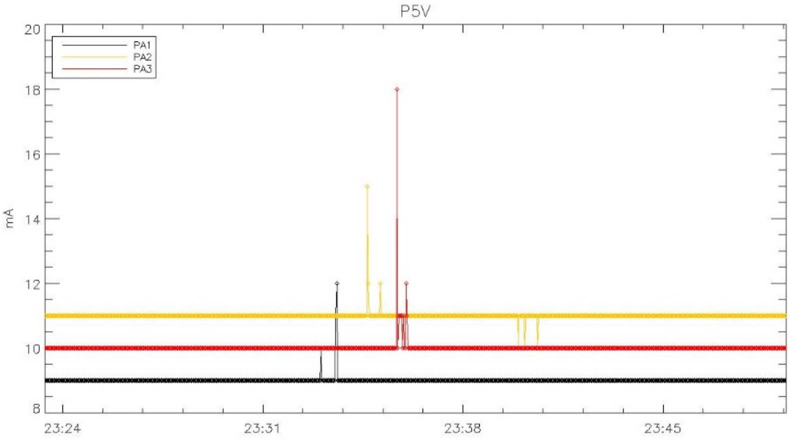

Figure 10. Current HK on the +5V of the 3 PA HF.

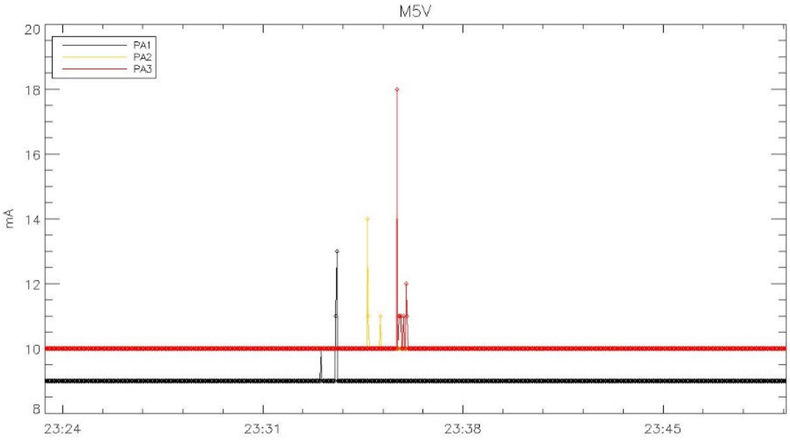

Figure 11. Current HK on the -5V of the 3 PA HF.

Observation:

- Overconsumption of HF preamps is clearly observed at the precise moment when the breakdown occurs.
- This overconsumption results in more or less intense current peaks, which spread over approximately 1 min.
- The currents on the +/-5V voltages of the 3 HF preamps are very correlated, which is rather normal.
- By fluctuating from 10 to 18mA, the preamps #3 has a higher consumption peak than the other 2 preamps.
- Consumption transients of this type have already been observed at other times but not with such intensity (see [RD2]).
- Consumption always ends up returning to its original level (~10mA)

The origin of these consumption peaks seems to coincide with the high voltage (HV) sweep (+/- 60V) of BIAS. They are not a priori caused by external events; e.g. impacts of charged particles on the antennas.

Everything happens as if the HV sweep created a high level AC signal, which by interfering with the input of the HF preamps, would cause them to overconsume. However, the reason why HV sweep generates such a spurious signal at such a high level is not understood (intrinsic to the experiment, interaction with the plasma, voltage breakdown?)
The consumption returns to its original level. This suggests that the HF preamps are not damaged and in good health (this is a necessary condition but may be not sufficient).
Note: The time resolution of the HK is probably too low to have a good restitution of the overconsumption profile.

3.2.4.3 Behavior after failure

Type III signals were observed after the breakdown. These are characterized by broadband emissions whose spectrum changes over time. They cover practically the entire range of TNR BCD bands (16 kHz to 1 MHz); which allows us to see the behavior of the instrument over a relatively wide spectral range.

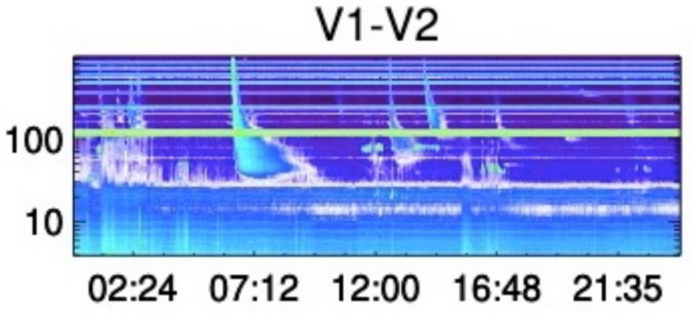

Figure 12. Dynamical spectrum acquired by TNR in V1-V2 dipole on Jan. 22, 2024.

We then see that it is still possible to see a type III residue on ANT#3 at the high frequencies of the TNR only; which is absolutely not the case at the lowest frequencies. The following figure illustrates this observation on the 634 kHz channel.

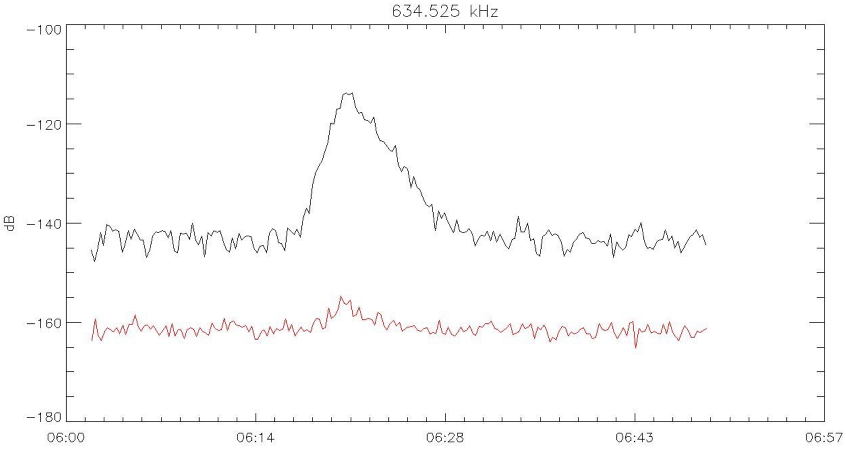

Figure 13. Type III observed on the TNR at 634.525 kHz (V1-V2 in black and V3 in red).

This observation shows that the signal on V3 is attenuated by around 40 dB compared to that measured on V1-V2. It is very weak but it does exist and this is not due to crosstalk because

the inter-channel isolation is much higher than 40 dB (to be confirmed with the ground calibration data).
It should also be taken into account that the V1-V2 dipole captures approximately twice as much signal as the V3 monopole, which reduces the attenuation to ~35 dB. This nevertheless remains a very rough approximation because we do not take into account here the orientation of the antennas with respect to the source (antennas parallel to the wavefront capture much more signal than when they are perpendicular to it)

3.2.4.4 Rough estimation of short circuit impedance

The normal attenuation due to the combination of antenna capacitance and base capacitance is:

$$\Gamma = \frac{C_A}{C_A + C_B}$$

We show that if we insert a resistor, R_B, in parallel with C_B (to model the short circuit), this attenuation becomes:

$$\Gamma' = \frac{jR_B C_A \omega}{1 + jR_B(C_A + C_B)\omega}$$

This equation raises a few remarks:

- Unlike Γ, Γ' is frequency dependent
- We see that this dependence decreases when ω increases
- I.e. $\Gamma' \rightarrow \Gamma$, when $\omega \rightarrow \infty$; which means that we get closer to a “normal” situation as the frequency increases
- We see that this is also the case when $R_B \rightarrow \infty$
- I.e. $\Gamma' \rightarrow \Gamma$ when the short circuit gradually disappears

Starting from this observation, **and accepting the hypothesis that the antennas are equally illuminated by the EM field**, it is possible to calculate an order of magnitude of the short circuit resistance (which is assumed but probable).
Indeed, we estimated the attenuation caused by the short circuit at 35 dB at the frequency of 634.525 kHz. On a linear scale, this corresponds to an attenuation factor $\alpha = 0{,}01778$ and $V_3 = \alpha V_{12}$. This can also result in the following relationship:

$$\|\Gamma'\|^2 = \|\alpha\Gamma\|^2$$

Where $\|*\|^2$ denotes the squared module of *.

It is then a matter of solving the following equation to express R_B as a function of the other parameters:

$$\frac{[R_B C_A \omega]^2}{1 + [R_B(C_A + C_B)\omega]^2} = \alpha^2 \left[\frac{C_A}{C_A + C_B}\right]^2$$

After simplification:

$$\frac{[R_B(C_A + C_B)\omega]^2}{1 + [R_B(C_A + C_B)\omega]^2} = \alpha^2$$

Finally:

$$R_B = \sqrt{\frac{\alpha^2}{(1-\alpha^2)(C_A + C_B)^2\omega^2}} = \frac{\alpha}{\sqrt{1-\alpha^2}} \frac{1}{(C_A + C_B)\omega}$$

We note that if $\alpha = 1$ (i.e. without the attenuation caused by the breakdown) $R_B \rightarrow \infty$, which corresponds to an open circuit.

From this result, and knowing the values of C_A, C_B and α at $f = 634.525\ kHz$, we calculate R_B.

We estimate C_A using the approximation commonly used for short antennas, where their impedance is comparable to a capacitance (the contribution of the resistive term is negligible). Under these conditions, the capacity of a cylindrical monopole of length, L, and radius, a, is:

$$C_A \approx \frac{2\pi\varepsilon_0 L}{ln(L/a) - 1}$$

Taking $L = 650\ cm$ and $a = 1\ cm$, we have $C_A \approx 66\ pF$. And assuming that $C_B \approx 50\ pF$, we obtain $R_B \approx 38.5\ \Omega$.

To have an idea of the sensitivity of R_B to the dispersions of $C_A + C_B$ and of α, we calculate it for different values of these parameters:

Case	$C_A + C_B$ (pF)	α (dB)	R_B (Ω)
1	116	35	38.5
2	116	30	68.4
3	116	40	21.6
4	116*50%	35	76.9
5	116/50%	35	19.2

Table 1. C_A+C_B dispersion sensitivity R_B cases

This shows that R_B varies in a relatively small range even with significant fluctuation in other parameters.

Furthermore, if the short circuit is in the format of a thin filament (of great length compared to the diameter), it cannot be excluded that its impedance is resistive and inductive (RL series). In this case, the release of the short circuit will be even more pronounced at HF.

NOTE: Bias team mentions the short when it was initially active showed a resistance to ground of about 37-40 ohm and once it started to work again showed ~500Mohm at one instance (this is from a sweep on 6 March were the Bias team could see a slope of 2uA in about 1V).

3.2.4.5 HFR measurements

It would have been interesting to extend the observations into the HFR range (400 kHz – 16 MHz). However, HFR does not provide V3 access. In this case, the combination of antennas is limited to dipoles:

- V12 = V1-V2
- V23 = V2-V3
- V31 = V3-V1

Unfortunately, this system of equations is not invertible and therefore does not allow V3 to be expressed as a function of dipole measurements.

3.2.5 HF Preamplifiers (PA)

Analysis have been performed by RPW CNES team [RD3] and THR team at LESIA (see 7.5) about a risk of latch-up in the HF PA electronics during Bias sweeps.

Main conclusion is the ANT3 failure is not due to HF PA latch-up. Nevertheless, current table used for Bias sweeps includes “hard” voltage transients, which may prematurely age the HF PA electronics. Decision has been hence taken to use “smoothed” Bias sweep table on-board (see section 5.1.2).

1.1.1 Plateform

No special event was reported by ESA at the S/C level during the anomaly occurrence time. Nevertheless Chris Watson (SOC) has noticed that the anomaly occurred during a S/C attitude disturbance event (SLEW).

1.1.2 Other instruments

No special event was reported by MAG, SWA and EPD teams around the anomaly occurrence time.

3.3 Possible root causes

Table below gives the list of possible root causes, with the pro/con arguments.

The most probable cause envisaged by RPW team at this stage of the investigation is indicated with bold characters.

CAUSE	INITIAL JUSTIFICATION(S)	PROS	CONS
“Ground” element in contact with the antenna	**An “ground” element in contact with the antenna can create a short** **Element could be floating MLI/SLI (glue problem?) or PA box part (small top doors used to free the stacer during antenna deployment?)**	**All the observations reported in section 3.2 can be compatible with a short caused by an S/C body or PA box element in contact with the ANT3**	
Direct impact by dust or micrometeorit	Dust impacts were reported on November 13, 2023. It is known from previous space missions that micrometeorits can damage antennas (cf. Wind/Waves X dipole was broken twice during the mission on 2000 and 2002).		After verification, the dust impact occurred earlier on November 13. No dust impact observed in the data during anomaly Direct impact should cause irreversible damage

			Direct impact may not impact both LF and HF signals RPW antenna diameter (3.8 cm) is large (compared to the diameter of Wind/Waves antennas: 0.04 cm). The risk of break by micrometeorits is very low here.
Spacecraft 'debris' caused by dust impacts	Stuart Bale (PSP/FIELDS PI) reported a Bias anomaly on FIELDS due Spacecraft heatshield 'debris' being catched by antennas 1 and 2[1]. SoloHI images let think the Solar Orbiter heatshield also released 'debris' (see image in appendix 7.7) Do accumulated debris could cause a short with ANT3?		No direct observation of such \`debris\` has been reported on RPW. Analysis of SoloHi images may help to confirm it. Anomaly occurred suddently Setting Bias current for ANT3 to +10 uA did not permit to recover the nominal signal for ANT3
Energetic particle event		The peaks seen on the HF PA -+ 5V currents at the time of anomaly (Figures 10 and 11) could be caused by an energetic particle event. High enough energetic particle event could deteriorate the electronics	Energetic particle event should also be seen by other instruments, which was not the case. HF PA -+5V current peaks were already observed during bias sweeps in the past (see for instance in [RD2])

---

[1] FIELDS_Bias_07012021.pdf

Electronics failure	Short may cause by electronics failure	A failure at PCB level is still possible Risk of HF PA latch-up? (See CNES analysis in [RD3])	Anomaly is observed by all the analyzers TDS, LFR and HFR with acquisitions from both HF and LF channels According to THR and Bias teams, latch-up in HF PA is not the root cause of the failure (see 7.5)

Table 2. List of possible root causes

4 KNOWN IMPACTS

4.1 Hardware impact

No direct impact has been identified concerning the hardware of RPW (MEB and other sensors). From feedbacks received by SOC and other PI teams, the plateform and payload are not impacted too.

Nevertheless, as long as the root cause has not been clearly identified, actions have been taken to limit the risk, especially concerning the two other RPW antennas 1 (PZ) and 2 (PY) (see section 5 for more details).

4.2 Operational impact

There is no direct impact on the operational activities. However some operational instructions have been taken to avoid as much as possible acquisitions with the antenna 3 and to mitigate the risk to see the same failure happens to the two other RPW antennas (see section 5 for more details).

4.3 Science performance impact

4.3.1 Bias unit

Impact on science done with the Bias unit durig periods when ANT3 is shorten to ground is:

- 2D DC/LF electric field is no longer measured
- Only one component of DC/LF electric field is available

Otherwise, computing spacecraft potential and plasma density is fine using V1 only.

4.3.2 TDS

TDS has been switched to a monopole configuration (sampling the antennas individually), which is robust with respect to issues on one antenne. The basline dipole configuration used since the beginning of the mission is not very suitable, because, V3-V1 dipole measurement is more difficult to interpret when V3 signal is lost.

This configuration still allows to reconstruct two components of the electric field as before, but the noise and various interferences are more prominent in this mode, comparing to the dipole mode.

The overall impact of the anomaly on TDS science performance is thus relatively limited.

4.3.3 LFR

1. The BP1 spectral products combining two electric field components are no longer possible (radial component of the Poynting flux, phase velocity).
2. The onboard calibrated 5x5 spectral matrices BP2 and ASM have presently wrong electromagnetic crosscorrelations, as well as wrong electric autocorrelations, because the two electric field components used, V23_AC and V13_AC, are wrong.
3. For the same reason, the BP1 spectral product PE (trace power spectrum of the electric field) is presently wrong
4. By using back the V12_AC electric field component one may recover correct measurements of corresponding electromagnetic crosscorrelations and electric autocorrelations, so with just one electric field component instead of two. However, this will also require updating the kcoefficients used for the onboard calibration of spectral matrices, which has been implemented since LFR FSW update 3.3.0.16 (03/14/2023).

4.3.4 THR

- In HFR, measurements in dipole mode involing V3 is not possible anymore. Can be replaced by V1-V2 dipole.
- In TNR, measurements in monopole mode involing V3 is not possible anymore. Can be replaced by other antennas V1, V2.
- In TNR, the capability to perform goniopolarimetry measurements may be affected

4.4 Instrument data impact

- No impact known on HK data
- No valid science measurement possible with V3 on TNR-HFR data. Acquistions are performed with V1 and V2. Science data quality will be flagged to “degraded” during periods when failed V3 is used.
- No valid science measurement possible with V3 on TDS data. Acquistions are performed with V1 and V2. Science data quality will be flagged to “degraded” during periods when failed V3 is used.
- LFR science data strongly impacted with limited possible mitigations on-board (see section 4.3.3). Science data quality will be flagged to “degraded” during periods when V3 is failed.
- Bias science data impacted with limited possible mitigations on-board (see section 4.3.1). Especially, only component of the E-field can be measured with only two antennas (nevertheless, according to Bias team, it might be still possible to derive the plasma local density). Science data quality will be flagged to “degraded” during periods when V3 is failed.

5 ACTIONS TAKEN

5.1 Failure isolation and risk mitigations

5.1.1 Failure isolation

Antenna failure cannot be isolated at this stage. Nevertheless, when it is possible, the configurations of the analyzers can be changed to avoid measurements with the antenna 3.

Since no direct risk has been identified, the ANT3 HF and LF PAs remain ON for the moment.

Equipment	Applied setting	DOY of application
BIAS	Bias current set to +10 µA for antenna 3 during failure	Between 2024-022 (STP293) and 2024-060 (STP298)
	No regular Bias sweep using ANT3 (only once every 2-3 months)	Planned after mid-april 2024
LFR	Nothing done at this stage	
TDS	Use only antennas 1 and 2	2024-022 (STP293)
THR	Use only antennas 1 and 2	Already applied before the anomaly.

Table 3. Failure isolation related actions

NOTE: details of the configurations of RPW equipment is given in appendix 7.3.

5.1.2 Failure risk mitigations

The following actions have been taken to mitigate the risk when performing instrument operations on-board:

- No Bias sweep scheduled during S/C attitude manoeuvres (checked by operator from E-FECS. SOC also checks it on its side.)
- Reduce the rate of Bias sweeps, depending of the S/C-Sun distance (see Table 4)
- Perform Bias sweep on ANT3 only once every 2-3 months. A new sequence AIWF033T has been submitted to MOC. This sequence will be used to perform nominal Bias sweeps on the ANT1 and ANT2, but with the parameter CP_BIA_SET_RELAY_BIA_3 {PIW00085} of TC_DPU_SET_BIAS_RELAY {ZIW00029} set to DISABLED, avoiding sweep with the ANT3[2]. Bias team should be able to define intensity current to be used for ANT3 from limited sweeps and from data acquired from ANT1 and ANT2 sweeps.
- Use a new "smoother" Bias sweep table values (see figure below) to limit the risk of damage for the HF PA (see section 3.2.5). The TC sequence required to load new Bias sweep table with TC_LOAD_BIAS_SWEEP {ZIW00060} command is in preparation.

---

[2] Succesful tests were performed on-board during Bias sweeps on March 13 and 15, 2024 to confirm that disabling relay for ANT3 is possible during a sweep. Tests done via PDOR.

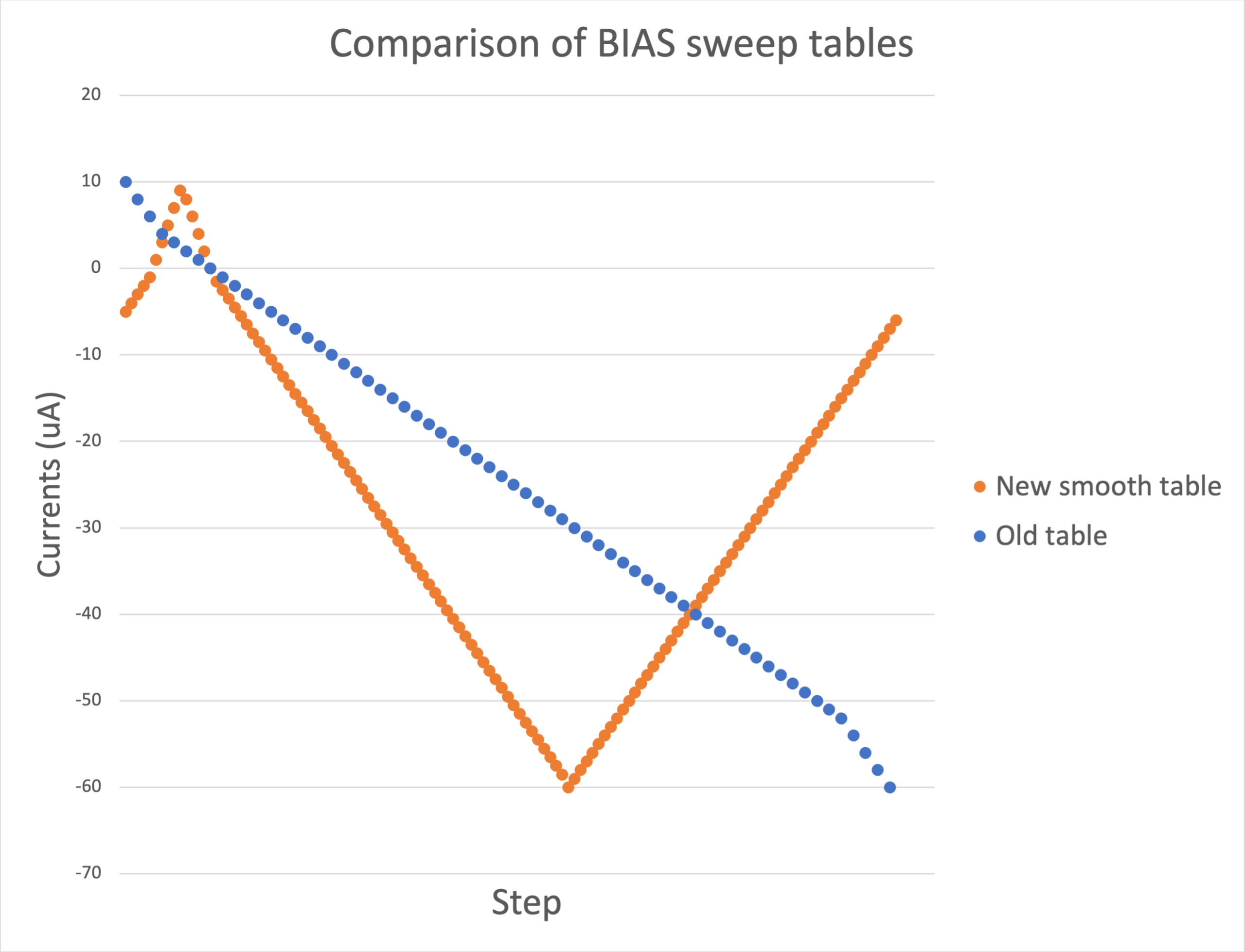

Figure 14. New Bias sweep table current values (orange dot) to be applied on-board to mitigate the HF PA latch-up during sweeps. Old table is plotted with blue dots.

Sweep occurrence rate	S/C-Sun distance (R) criterion
1 sweep / 5 day	0.4 AU < R < 0.7 AU
1 sweep / day	R < 0.4 AU
1 sweep / 5 day	0.4 AU < R < 0.7 AU
1 sweep / 10 day	0.7 AU < R

Table 4. Bias sweep rate occurrence rate as a function of S/C-Sun distance.

5.2 Ground segment

The following actions have been taken at ground segment level to mitigate the risk:

- Update operation instructions guide to take account of restrictions of activities permitted on-board (see list in section 5.1.2)

- Update IOR generation tool to notify operators when operation planning is not compliant with the restrictions (see list in section 5.1.2)
- Suspend temporary the delivery of RPW science data to SOAR, in order to indicate in the impacted CDF files when the anomaly occurred and what are the consequence(s) in terms of data quality
- Prepare and publish an anomaly report (current document)
- Plan with ESA, CNES and other RPW sub-system teams an anomaly review board (ARB). ARB is currently scheduled on April 26, 2024 at 9:30 (CEST).

6 RECOMMENDATIONS & FUTURE PLANS

6.1 In-flight diagnostic and recovery tests

UPDATE: Following recovery tests have been suspended for the moment, because the ANT3 signal has been back since February 28, 2023.

Test	Description	Justification	Date (if known)	Status
RPW equipment power cycle	A OFF/ON power cycle of RPW equipment	Test if the anomaly is due to electronics. A simple restart may the situation come to the normal		Suspended
Bias current test	Temporary increase the intensity of the Bias current injected in the antenna 3	If the ANT3 is shorten by an element (probably negatively charged) which is electrostatically attracted, injected a strong (positive) current may push back it away enough from the antenna.		Suspended

Table 5. In-flight diagnostic and recovery tests

6.2 Future plans

At this stage no more isolation/mitigation as well as diagnostic test activities are planned in the future. Activities relative to in-flight recovery tests are also suspended.

Data analysis by RPW team are continuing in order to understand why the antenna 3 was temporary lost then recovered.

Investigations about possible external causes (MLI, “debris” from heatshield, …) should be pursued too.

Current status and future plans will be discussed during ARB on April 26, 2024.

7 APPENDIX

7.1 Solar Orbiter E-FECS planning on November 13, 2023 around 23:36z

Figure below shows a extract of the E-FECS planning from the SoopKitchen tool for the LTP13.

Attitude disturbance (SLEW) was run between 23:36:00z and 23:41:00z when the anomaly occurred.

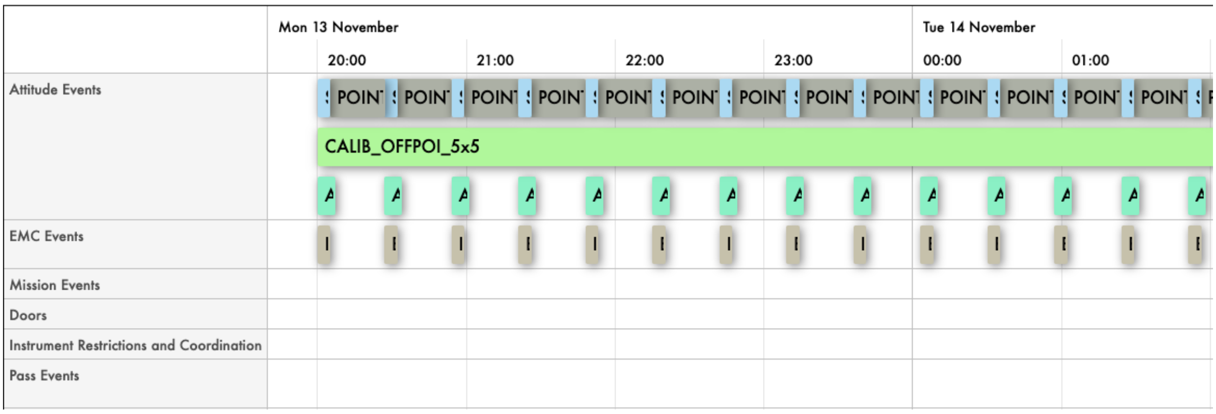

Figure 15. Mission level planning around Nov. 13, 2023 at 23:30z. (Extracted from LTP13_Sep2023-Dec2023 SoopKitchen plan). During this period, several attitude events were schedules: SLEW (in blue), POINT_PATTERN (in grey) and CALIB_OFFPOI_5x5.

7.2 RPW operation timeline on November 13, 2023 around 23:36z

Table below presents the timeline of RPW commands executed on-board between 23:32:00z and 23:39:16z on Nov. 13, 2023.

Name	Description	Stat. PTV	Dyn. PTV	MD	Execution Time	Parent Seq	Seq. Descr.
ZIW00094	TC_TDS_DUMP_NORMAL_TSWF			M	2023-317T23:32:00.000000	AIWF034B	Dump NORMAL TDS Triggered snapshots
PIW00251	CP_TDS_N_SNAPSHOTS_NR	Raw	FP:Dec	16			
PIW00252	CP_TDS_N_QUALITY	Raw	FP:Dec	0			
ZIW00036	TC_DPU_ENTER_SERVICE			M	2023-317T23:33:00.000000	AIWF043A	Enter SERVICE mode

ZIW00098	TC_TDS_LOAD_NORMAL_PAR			M	2023-317T23:33:03.000000	AIWF038N	Conf TDS Bias Sweep v15
PIW00297	SY_TDS_N_SAMP_RATE_RESERVED	Raw	Dec	0			
PIW00298	CP_TDS_N_SAMP_RATE	Def		SR_256			
PIW00299	SY_TDS_N_RS_RESERVED	Raw	Dec	0			
PIW00300	SY_TDS_N_RS_ENAB	Def		1			
PIW00301	CP_TDS_N_RS_ADC_CH_NR	Def		N_4_CH			
PIW00302	SY_TDS_N_RS_ADC_CH4	Def		1			
PIW00303	SY_TDS_N_RS_ADC_CH3	Def		1			
PIW00304	SY_TDS_N_RS_ADC_CH2	Def		1			
PIW00305	SY_TDS_N_RS_ADC_CH1	Def		1			
PIW00306	SY_TDS_N_HF_RESERVED	Def		0			
PIW01363	SY_TDS_N_AD4_HF2_LOAD	Def		0			
PIW01364	SY_TDS_N_AD3_HF2_LOAD	Def		0			
PIW01365	SY_TDS_N_AD2_HF1_LOAD	Def		0			
PIW01366	SY_TDS_N_AD1_HF3_LOAD	Def		0			
PIW00307	SY_TDS_N_HF_CH4_LOW_GAIN	Def		1			
PIW00308	SY_TDS_N_HF_CH4_INPUT_ENAB	Raw	Dec	0			
PIW00309	SY_TDS_N_HF_CH3_LOW_GAIN	Def		1			
PIW00310	SY_TDS_N_HF_CH3_INPUT_ENAB	Raw	Dec	0			
PIW00311	SY_TDS_N_HF_CH2_LOW_GAIN	Def		1			
PIW00312	SY_TDS_N_HF_CH2_INPUT_ENAB	Raw	Dec	0			
PIW00313	SY_TDS_N_HF_CH1_LOW_GAIN	Def		1			
PIW00314	SY_TDS_N_HF_CH1_INPUT_ENAB	Raw	Dec	0			
PIW00315	SY_TDS_N_AD4_MUXA_SET	Def		0			
PIW00316	SY_TDS_N_AD4_MUXA_INH	Def		0			
PIW00317	SY_TDS_N_AD4_MUXB_SET	Def		0			
PIW00318	SY_TDS_N_AD4_MUXB_INH	Def		1			

PIW00319	SY_TDS_N_AD3_MUXA_SET	Def		0			
PIW00320	SY_TDS_N_AD3_MUXA_INH	Def		0			
PIW00321	SY_TDS_N_AD3_MUXB_SET	Def		0			
PIW00322	SY_TDS_N_AD3_MUXB_INH	Def		1			
PIW00323	SY_TDS_N_AD2_MUXA_SET	Def		0			
PIW00324	SY_TDS_N_AD2_MUXA_INH	Def		0			
PIW00325	SY_TDS_N_AD2_MUXB_SET	Def		0			
PIW00326	SY_TDS_N_AD2_MUXB_INH	Def		1			
PIW00327	SY_TDS_N_AD1_MUXA_SET	Def		0			
PIW00328	SY_TDS_N_AD1_MUXA_INH	Def		0			
PIW00329	SY_TDS_N_AD1_MUXB_SET	Def		0			
PIW00330	SY_TDS_N_AD1_MUXB_INH	Def		1			
PIW00331	SY_TDS_N_RS_DELAY_COARSE	Raw	Dec	600			
PIW00332	SY_TDS_N_RS_DELAY_FINE	Def		0			
PIW00333	SY_TDS_N_RS_LEN	Def		NSAMP_4K			
PIW00334	SY_TDS_N_FILTERS	Eng		FILTER_SET2			
PIW00335	SY_TDS_N_TS_RESERVED	Raw	Dec	0			
PIW00336	SY_TDS_N_TS_ENAB	Raw	Dec	0			
PIW00337	CP_TDS_N_TS_ADC_CH_NR	Def		N_4_CH			
PIW00338	SY_TDS_N_TS_ADC_CH4	Def		1			
PIW00339	SY_TDS_N_TS_ADC_CH3	Def		1			
PIW00340	SY_TDS_N_TS_ADC_CH2	Def		1			
PIW00341	SY_TDS_N_TS_ADC_CH1	Def		1			
PIW01163	SY_TDS_N_TS_PERIOD_COARSE	Def		1			
PIW01164	SY_TDS_N_TS_PERIOD_FINE	Def		0			
PIW01165	SY_TDS_N_TS_LEN	Def		NSAMP_16K			
PIW00343	SY_TDS_N_QUEUE_LEN	Def		16			

PIW00344	SY_TDS_N_STAT_DATA_PERIOD	Def		16			
PIW00345	SY_TDS_N_1D_HIST_PERIOD	Def		600			
PIW00346	SY_TDS_N_2D_HIST_PERIOD	Def		1800			
PIW00347	CP_TDS_N_STAT_DATA	Eng		STAT_DISABLE			
PIW01367	SY_TDS_N_MAMP_ENAB	Def		0			
PIW01368	SY_TDS_N_MAMP_DEC_RATE	Def		MAMP_DEC_1X			
PIW01369	SY_TDS_N_MAMP_ADC_CH4	Def		1			
PIW01370	SY_TDS_N_MAMP_ADC_CH3	Def		1			
PIW01371	SY_TDS_N_MAMP_ADC_CH2	Def		1			
PIW01372	SY_TDS_N_MAMP_ADC_CH1	Def		1			
PIW00349	CP_TDS_N_1D_HIST1_TYPE	Eng		DISABLED			
PIW01390	CP_TDS_N_1D_HIST1_AXIS	Def		LOG_HIST_128			
PIW00350	CP_TDS_N_1D_HIST2_TYPE	Eng		DISABLED			
PIW01391	CP_TDS_N_1D_HIST2_AXIS	Def		HISTA_128			
PIW00351	CP_TDS_N_1D_HIST3_TYPE	Eng		DISABLED			
PIW01392	CP_TDS_N_1D_HIST3_AXIS	Def		LOG_HIST_128			
PIW00352	CP_TDS_N_1D_HIST4_TYPE	Eng		DISABLED			
PIW01393	CP_TDS_N_1D_HIST4_AXIS	Def		LOG_HIST_256			
PIW00353	CP_TDS_N_2D_HIST1_TYPE	Eng		DISABLED			
PIW00354	CP_TDS_N_2D_HIST1_X_AXIS	Eng		HISTA_128			
PIW00355	CP_TDS_N_2D_HIST1_Y_AXIS	Eng		LOG_HIST_32			
PIW00356	CP_TDS_N_2D_HIST2_TYPE	Def		DISABLED			
PIW00357	CP_TDS_N_2D_HIST2_X_AXIS	Eng		HISTA_128			
PIW00358	CP_TDS_N_2D_HIST2_Y_AXIS	Eng		HISTA_128			
PIW00359	SY_TDS_N_STAT_PAR_THRESHOLD	Def		100			
PIW00360	CP_TDS_ALGO_SELECTION	Def		BEST_WAVES			
PIW00361	SY_TDS_ALGO_DUST_NUM	Def		1			

PIW00362	SY_TDS_ALGO_MIN_QUALITY	Def		0			
PIW00363	SY_TDS_ALGO_CHANNEL	Def		ADC1			
PIW00364	SY_TDS_ALGO_STAT_ADC4	Def		0			
PIW00365	SY_TDS_ALGO_STAT_ADC3	Def		1			
PIW00366	SY_TDS_ALGO_STAT_ADC2	Def		1			
PIW00367	SY_TDS_ALGO_STAT_ADC1	Def		1			
PIW00368	SY_TDS_ALGO_MIN_AMP	Def		64			
PIW00369	SY_TDS_ALGO_THRESH_WAVE	Def		80000000			
PIW00370	SY_TDS_ALGO_THRESH_DUST	Raw	Dec	56000000			
PIW00371	SY_TDS_ALGO_THRESH_EX	Def		16384			
PIW00372	SY_TDS_ALGO_PARAM1	Def		0			
PIW00373	SY_TDS_ALGO_PARAM2	Def		0			
ZIW00029	TC_DPU_SET_BIAS_RELAY			M	2023-317T23:33:04.000000	AIWF033O	Run BIAS sweep 1 v19
PIW00076	CP_BIA_COMMAND_NAME	Eng		SET_RELAY			
PIW01347	CP_BIA_SET_RELAY_DIFF_GAIN	Raw	FP:Eng	GAIN_5			
PIW00085	CP_BIA_SET_RELAY_BIA_3	Eng		ENABLED			
PIW00086	CP_BIA_SET_RELAY_BIA_2	Eng		ENABLED			
PIW00087	CP_BIA_SET_RELAY_BIA_1	Eng		ENABLED			
PIW00088	CP_BIA_SET_RELAY_DIFF_PROBE	Raw	FP:Eng	DIFF_PR1_PR3			
PIW00089	CP_BIA_SET_RELAY_SWITCH_P3	Raw	FP:Eng	NOT_SELECTED			
PIW00090	CP_BIA_SET_RELAY_SWITCH_P2	Raw	FP:Eng	NOT_SELECTED			
PIW00091	CP_BIA_SET_RELAY_SWITCH_P1	Raw	FP:Eng	NOT_SELECTED			
ZIW00027	TC_DPU_SET_BIAS_MODE			M	2023-317T23:33:08.000000	AIWF033O	Run BIAS sweep 1 v19
PIW00076	CP_BIA_COMMAND_NAME	Eng		SET_MODE			
PIW00080	CP_BIA_SET_MODE_ENAB_SET_HV	Eng		ENABLED			
PIW00081	CP_BIA_SET_MODE_ENAB_HV	Eng		ENABLED			

PIW00082	CP_BIA_SET_MODE_ENAB_SET_MX	Eng		ENABLED			
PIW00083	CP_BIA_SET_MODE_SET_MX_MODE	Eng		MUX_4			
ZIW00077	TC_LFR_LOAD_COMMON_PAR			M	2023-317T23:33:11.000000	AIWF033O	Run BIAS sweep 1 v19
PIW00230	SY_LFR_BW	Def		1			
PIW00231	SY_LFR_SP0	Def		0			
PIW00232	SY_LFR_SP1	Def		0			
PIW00233	SY_LFR_R0	Raw	Dec	1			
PIW00234	SY_LFR_R1	Raw	Dec	1			
PIW01348	SY_LFR_R2	Raw	Dec	1			
ZIW00037	TC_DPU_ENTER_SURVEY_NORMAL			M	2023-317T23:33:12.000000	AIWF033O	Run BIAS sweep 1 v19
PIW01293	CP_DPU_ABSOLUTE_SYNC_FLAG	Def		0			
ZIW00062	TC_DPU_START_BIAS_SWEEP			M	2023-317T23:33:14.000000	AIWF033O	Run BIAS sweep 1 v19
PIW01360	CP_DPU_BIAS_SWEEP_TRACE	Raw	FP:Dec	0			
PIW00220	CP_DPU_BIA_SWEEP_ANT_1_CUR	Raw	FP:Eng	0			
PIW00221	CP_DPU_BIA_SWEEP_ANT_2_CUR	Raw	FP:Eng	0			
PIW00222	CP_DPU_BIA_SWEEP_ANT_3_CUR	Raw	FP:Eng	0			
PIW01301	CP_DPU_BIA_SWEEP_DURATION	Raw	FP:Dec	1			
ZIW00036	TC_DPU_ENTER_SERVICE			M	2023-317T23:39:05.000000	AIWF033I	Configure and execute the BIAS sweep Part 3
ZIW00027	TC_DPU_SET_BIAS_MODE			M	2023-317T23:39:08.000000	AIWF033I	Configure and execute the BIAS sweep Part 3
PIW00076	CP_BIA_COMMAND_NAME	Eng		SET_MODE			
PIW00080	CP_BIA_SET_MODE_ENAB_SET_HV	Eng		ENABLED			
PIW00081	CP_BIA_SET_MODE_ENAB_HV	Eng		ENABLED			
PIW00082	CP_BIA_SET_MODE_ENAB_SET_MX	Eng		ENABLED			
PIW00083	CP_BIA_SET_MODE_SET_MX_MODE	Eng		MUX_0			

ZIW00077	TC_LFR_LOAD_COMMON_PAR			M	2023-317T23:39:11.000000	AIWF033I	Configure and execute the BIAS sweep Part 3
PIW00230	SY_LFR_BW	Raw	FP:Dec	1			
PIW00231	SY_LFR_SP0	Raw	FP:Dec	0			
PIW00232	SY_LFR_SP1	Raw	FP:Dec	0			
PIW00233	SY_LFR_R0	Raw	FP:Dec	0			
PIW00234	SY_LFR_R1	Raw	FP:Dec	0			
PIW01348	SY_LFR_R2	Raw	FP:Dec	0			
ZIW00024	TC_DPU_SET_BIAS1			M	2023-317T23:39:12.000000	AIWF033I	Configure and execute the BIAS sweep Part 3
PIW00076	CP_BIA_COMMAND_NAME	Eng		SET_BIAS1			
PIW00077	CP_BIA_SET_BIAS1	Raw	FP:Eng	-3.000000			
ZIW00025	TC_DPU_SET_BIAS2			M	2023-317T23:39:13.000000	AIWF033I	Configure and execute the BIAS sweep Part 3
PIW00076	CP_BIA_COMMAND_NAME	Eng		SET_BIAS2			
PIW00078	CP_BIA_SET_BIAS2	Raw	FP:Eng	-3.500000			
ZIW00026	TC_DPU_SET_BIAS3			M	2023-317T23:39:14.000000	AIWF033I	Configure and execute the BIAS sweep Part 3
PIW00076	CP_BIA_COMMAND_NAME	Eng		SET_BIAS3			
PIW00079	CP_BIA_SET_BIAS3	Raw	FP:Eng	-3.400000			
ZIW00098	TC_TDS_LOAD_NORMAL_PAR			M	2023-317T23:39:15.000000	AIWF038M	TDS configuration for normal mode - XLD
PIW00297	SY_TDS_N_SAMP_RATE_RESERVED	Raw	Dec	0			
PIW00298	CP_TDS_N_SAMP_RATE	Raw	FP:Eng	SR_256			
PIW00299	SY_TDS_N_RS_RESERVED	Raw	Dec	0			
PIW00300	SY_TDS_N_RS_ENAB	Raw	FP:Dec	1			
PIW00301	CP_TDS_N_RS_ADC_CH_NR	Raw	FP:Eng	N_2_CH			
PIW00302	SY_TDS_N_RS_ADC_CH4	Raw	FP:Dec	0			
PIW00303	SY_TDS_N_RS_ADC_CH3	Raw	FP:Dec	0			

PIW00304	SY_TDS_N_RS_ADC_CH2	Raw	FP:Dec	1			
PIW00305	SY_TDS_N_RS_ADC_CH1	Raw	FP:Dec	1			
PIW00306	SY_TDS_N_HF_RESERVED	Def		0			
PIW01363	SY_TDS_N_AD4_HF2_LOAD	Def		0			
PIW01364	SY_TDS_N_AD3_HF2_LOAD	Def		0			
PIW01365	SY_TDS_N_AD2_HF1_LOAD	Def		0			
PIW01366	SY_TDS_N_AD1_HF3_LOAD	Raw	Dec	1			
PIW00307	SY_TDS_N_HF_CH4_LOW_GAIN	Raw	FP:Dec	0			
PIW00308	SY_TDS_N_HF_CH4_INPUT_ENAB	Def		1			
PIW00309	SY_TDS_N_HF_CH3_LOW_GAIN	Raw	FP:Dec	1			
PIW00310	SY_TDS_N_HF_CH3_INPUT_ENAB	Def		1			
PIW00311	SY_TDS_N_HF_CH2_LOW_GAIN	Raw	FP:Dec	1			
PIW00312	SY_TDS_N_HF_CH2_INPUT_ENAB	Def		1			
PIW00313	SY_TDS_N_HF_CH1_LOW_GAIN	Raw	FP:Dec	1			
PIW00314	SY_TDS_N_HF_CH1_INPUT_ENAB	Def		1			
PIW00315	SY_TDS_N_AD4_MUXA_SET	Def		0			
PIW00316	SY_TDS_N_AD4_MUXA_INH	Def		0			
PIW00317	SY_TDS_N_AD4_MUXB_SET	Def		0			
PIW00318	SY_TDS_N_AD4_MUXB_INH	Def		1			
PIW00319	SY_TDS_N_AD3_MUXA_SET	Def		0			
PIW00320	SY_TDS_N_AD3_MUXA_INH	Raw	Dec	1			
PIW00321	SY_TDS_N_AD3_MUXB_SET	Def		0			
PIW00322	SY_TDS_N_AD3_MUXB_INH	Raw	Dec	0			
PIW00323	SY_TDS_N_AD2_MUXA_SET	Def		0			
PIW00324	SY_TDS_N_AD2_MUXA_INH	Def		0			
PIW00325	SY_TDS_N_AD2_MUXB_SET	Def		0			
PIW00326	SY_TDS_N_AD2_MUXB_INH	Raw	Dec	0			

PIW00327	SY_TDS_N_AD1_MUXA_SET	Def		0			
PIW00328	SY_TDS_N_AD1_MUXA_INH	Def		0			
PIW00329	SY_TDS_N_AD1_MUXB_SET	Raw	Dec	1			
PIW00330	SY_TDS_N_AD1_MUXB_INH	Raw	Dec	0			
PIW00331	SY_TDS_N_RS_DELAY_COARSE	Raw	FP:Dec	15			
PIW00332	SY_TDS_N_RS_DELAY_FINE	Def		0			
PIW00333	SY_TDS_N_RS_LEN	Raw	FP:Eng	NSAMP_16K			
PIW00334	SY_TDS_N_FILTERS	Raw	FP:Eng	FILTER_SET3			
PIW00335	SY_TDS_N_TS_RESERVED	Raw	Dec	0			
PIW00336	SY_TDS_N_TS_ENAB	Raw	FP:Dec	1			
PIW00337	CP_TDS_N_TS_ADC_CH_NR	Def		N_4_CH			
PIW00338	SY_TDS_N_TS_ADC_CH4	Def		1			
PIW00339	SY_TDS_N_TS_ADC_CH3	Def		1			
PIW00340	SY_TDS_N_TS_ADC_CH2	Def		1			
PIW00341	SY_TDS_N_TS_ADC_CH1	Def		1			
PIW01163	SY_TDS_N_TS_PERIOD_COARSE	Def		1			
PIW01164	SY_TDS_N_TS_PERIOD_FINE	Def		0			
PIW01165	SY_TDS_N_TS_LEN	Raw	FP:Eng	NSAMP_16K			
PIW00343	SY_TDS_N_QUEUE_LEN	Raw	FP:Dec	16			
PIW00344	SY_TDS_N_STAT_DATA_PERIOD	Raw	FP:Dec	16			
PIW00345	SY_TDS_N_1D_HIST_PERIOD	Raw	FP:Dec	600			
PIW00346	SY_TDS_N_2D_HIST_PERIOD	Raw	FP:Dec	1800			
PIW00347	CP_TDS_N_STAT_DATA	Raw	FP:Eng	STAT_ENABLE			
PIW01367	SY_TDS_N_MAMP_ENAB	Raw	FP:Dec	1			
PIW01368	SY_TDS_N_MAMP_DEC_RATE	Raw	FP:Eng	MAMP_DEC_1X			
PIW01369	SY_TDS_N_MAMP_ADC_CH4	Raw	FP:Dec	1			
PIW01370	SY_TDS_N_MAMP_ADC_CH3	Raw	FP:Dec	1			

PIW01371	SY_TDS_N_MAMP_ADC_CH2	Raw	FP:Dec	1			
PIW01372	SY_TDS_N_MAMP_ADC_CH1	Raw	FP:Dec	1			
PIW00349	CP_TDS_N_1D_HIST1_TYPE	Raw	FP:Eng	PEAK_W_AMP			
PIW01390	CP_TDS_N_1D_HIST1_AXIS	Raw	FP:Eng	LOG_HIST_128			
PIW00350	CP_TDS_N_1D_HIST2_TYPE	Raw	FP:Eng	WAVE_FREQ			
PIW01391	CP_TDS_N_1D_HIST2_AXIS	Raw	FP:Eng	HISTA_128			
PIW00351	CP_TDS_N_1D_HIST3_TYPE	Raw	FP:Eng	RMS_S_AMP			
PIW01392	CP_TDS_N_1D_HIST3_AXIS	Raw	FP:Eng	LOG_HIST_128			
PIW00352	CP_TDS_N_1D_HIST4_TYPE	Raw	FP:Eng	MAXAMP_CH1			
PIW01393	CP_TDS_N_1D_HIST4_AXIS	Raw	FP:Eng	LOG_HIST_256			
PIW00353	CP_TDS_N_2D_HIST1_TYPE	Raw	FP:Eng	DA_VS_RE			
PIW00354	CP_TDS_N_2D_HIST1_X_AXIS	Raw	FP:Eng	HISTA_128			
PIW00355	CP_TDS_N_2D_HIST1_Y_AXIS	Raw	FP:Eng	LOG_HIST_32			
PIW00356	CP_TDS_N_2D_HIST2_TYPE	Raw	FP:Eng	WA_RMS_VS_FQ			
PIW00357	CP_TDS_N_2D_HIST2_X_AXIS	Raw	FP:Eng	LOG_HIST_128			
PIW00358	CP_TDS_N_2D_HIST2_Y_AXIS	Raw	FP:Eng	LOG_HIST_128			
PIW00359	SY_TDS_N_STAT_PAR_THRESHOLD	Raw	FP:Dec	1200			
PIW00360	CP_TDS_ALGO_SELECTION	Raw	FP:Eng	BEST_WAVES			
PIW00361	SY_TDS_ALGO_DUST_NUM	Raw	FP:Dec	2			
PIW00362	SY_TDS_ALGO_MIN_QUALITY	Def		0			
PIW00363	SY_TDS_ALGO_CHANNEL	Raw	FP:Eng	ADC2			
PIW00364	SY_TDS_ALGO_STAT_ADC4	Def		0			
PIW00365	SY_TDS_ALGO_STAT_ADC3	Def		1			
PIW00366	SY_TDS_ALGO_STAT_ADC2	Def		1			
PIW00367	SY_TDS_ALGO_STAT_ADC1	Def		1			
PIW00368	SY_TDS_ALGO_MIN_AMP	Raw	FP:Dec	120			
PIW00369	SY_TDS_ALGO_THRESH_WAVE	Raw	FP:Dec	10000			

PIW00370	SY_TDS_ALGO_THRESH_DUST	Raw	FP:Dec	2800			
PIW00371	SY_TDS_ALGO_THRESH_EX	Raw	FP:Dec	17151104			
PIW00372	SY_TDS_ALGO_PARAM1	Raw	FP:Dec	0			
PIW00373	SY_TDS_ALGO_PARAM2	Raw	FP:Dec	8553298			
ZIW00040	TC_DPU_ENTER_SBM_DETECTION			M	2023-317T23:39:16.000000	AIWF035C	Enter SBM_DETECTION mode
PIW01293	CP_DPU_ABSOLUTE_SYNC_FLAG	Raw	FP:Dec	1			

Table 6. RPW commands executed on-board between 23:32:00z and 23:39:16z on Nov. 13, 2023

7.3 Instrument configurations applied on-board to reduce the impact on science performance

Table below gives the main changes of configuration of sub-systems applied in science modes for mitigate the impact of the anomaly. Changes are presented in terms of sequences, TC and formal parameter (FP) values.

Equipment	Configurations
BIAS	• CP_BIAS_SET_MODE_SET_MX_MODE{PIW00083} = MUX_4 • CP_BIA_SET_BIAS3{PIW00079} = +10 µA
LFR	No change. Sensor setting is performed via Bias TC
TDS	NORMAL -- Use AIWF038K with: • CP_TDS_N_SAMP_RATE [PIW00298] = SR_256 • CP_TDS_N_RS_ADC_CH_NR [PIW00301] = N_4_CH (not a FP) • SY_TDS_N_RS_ADC_CH4 [PIW00302] = 1 (not a FP) • SY_TDS_N_RS_ADC_CH3 [PIW00303] = 1 (not a FP) • SY_TDS_N_RS_ADC_CH2 [PIW00304] = 1 (not a FP) • SY_TDS_N_RS_ADC_CH1 [PIW00305] = 1 (not a FP) • SY_TDS_N_HF_CH4_LOW_GAIN [PIW00307] = 0 • SY_TDS_N_RS_DELAY_COARSE [PIW00331] = 3600 • SY_TDS_N_RS_LEN [PIW00333] = NSAMP_8K • SY_TDS_N_FILTERS [PIW00334] = FILTER_SET3 • SY_TDS_N_STAT_PAR_THRESHOLD [PIW00359] = 1200 • SY_TDS_ALGO_DUST_NUM [PIW00361] = 2 • SY_TDS_ALGO_CHANNEL [PIW00363] = ADC1 • SY_TDS_ALGO_MIN_AMP [PIW00368] = 120 • SY_TDS_ALGO_THRESH_WAVE [PIW00369] = 10000 • SY_TDS_ALGO_THRESH_DUST [PIW00370] = 2800 • SY_TDS_ALGO_THRESH_EX [PIW00371] = 17151004 • SY_TDS_ALGO_PARAM1 [PIW00372] = 0 • SY_TDS_ALGO_PARAM2 [PIW00373] = 8553298 • SY_TDS_N_MAMP_DEC_RATE [PIW01368] = MAMP_DEC_1X

<table>
<tr><td></td><td>BURST -- Use AIWF038F with :
• CP_TDS_B_RS_ADC_CH_NR [PIW00376] = N_4_CH
• SY_TDS_B_RS_DELAY_COARSE [PIW00381] = 3600
• SY_TDS_B_RS_LEN [PIW00383] = NSAMP_8K
• SY_TDS_B_RS_ADC_CH4 [PIW00377] = 1
• SY_TDS_B_RS_ADC_CH3 [PIW00378] = 1
• SY_TDS_B_RS_ADC_CH2 [PIW00379] = 1
• SY_TDS_B_RS_ADC_CH1 [PIW00380] = 1
• SY_TDS_B_MAMP_DEC_RATE [PIW01374] = MAMP_DEC_1X</td></tr>
<tr><td>THR</td><td>
<table>
<tr><td>ZIW00112</td><td>TC_THR_LOAD_NORMAL_PAR_1</td><td>M</td><td>AIWF037J</td></tr>
<tr><td>PIW01402</td><td>SY_THR_N_TS_SEQ_POS</td><td>1</td><td></td></tr>
<tr><td>PIW00462</td><td>SY_THR_N_SET_TS_AV</td><td>NR_AV_16</td><td></td></tr>
<tr><td>PIW00463</td><td>SY_THR_N_SET_TS_CR</td><td>DISABLED</td><td></td></tr>
<tr><td>PIW00464</td><td>SY_THR_N_SET_TS_AU</td><td>ENABLED</td><td></td></tr>
<tr><td>PIW00465</td><td>SY_THR_N_SET_TS_BAND_D</td><td>1</td><td></td></tr>
<tr><td>PIW00466</td><td>SY_THR_N_SET_TS_BAND_C</td><td>1</td><td></td></tr>
<tr><td>PIW00467</td><td>SY_THR_N_SET_TS_BAND_B</td><td>1</td><td></td></tr>
<tr><td>PIW00468</td><td>SY_THR_N_SET_TS_BAND_A</td><td>1</td><td></td></tr>
<tr><td>PIW01402</td><td>SY_THR_N_TS_SEQ_POS</td><td>0</td><td></td></tr>
<tr><td>PIW00462</td><td>SY_THR_N_SET_TS_AV</td><td>NR_AV_32</td><td></td></tr>
<tr><td>PIW00463</td><td>SY_THR_N_SET_TS_CR</td><td>DISABLED</td><td></td></tr>
<tr><td>PIW00464</td><td>SY_THR_N_SET_TS_AU</td><td>DISABLED</td><td></td></tr>
<tr><td>PIW00465</td><td>SY_THR_N_SET_TS_BAND_D</td><td>1</td><td></td></tr>
<tr><td>PIW00466</td><td>SY_THR_N_SET_TS_BAND_C</td><td>1</td><td></td></tr>
<tr><td>PIW00467</td><td>SY_THR_N_SET_TS_BAND_B</td><td>1</td><td></td></tr>
<tr><td>PIW00468</td><td>SY_THR_N_SET_TS_BAND_A</td><td>1</td><td></td></tr>
<tr><td>PIW01402</td><td>SY_THR_N_TS_SEQ_POS</td><td>0</td><td></td></tr>
<tr><td>PIW00462</td><td>SY_THR_N_SET_TS_AV</td><td>NR_AV_32</td><td></td></tr>
<tr><td>PIW00463</td><td>SY_THR_N_SET_TS_CR</td><td>DISABLED</td><td></td></tr>
<tr><td>PIW00464</td><td>SY_THR_N_SET_TS_AU</td><td>DISABLED</td><td></td></tr>
<tr><td>PIW00465</td><td>SY_THR_N_SET_TS_BAND_D</td><td>1</td><td></td></tr>
<tr><td>PIW00466</td><td>SY_THR_N_SET_TS_BAND_C</td><td>1</td><td></td></tr>
<tr><td>PIW00467</td><td>SY_THR_N_SET_TS_BAND_B</td><td>1</td><td></td></tr>
<tr><td>PIW00468</td><td>SY_THR_N_SET_TS_BAND_A</td><td>1</td><td></td></tr>
<tr><td>PIW01402</td><td>SY_THR_N_TS_SEQ_POS</td><td>0</td><td></td></tr>
<tr><td>PIW00462</td><td>SY_THR_N_SET_TS_AV</td><td>NR_AV_32</td><td></td></tr>
<tr><td>PIW00463</td><td>SY_THR_N_SET_TS_CR</td><td>DISABLED</td><td></td></tr>
<tr><td>PIW00464</td><td>SY_THR_N_SET_TS_AU</td><td>DISABLED</td><td></td></tr>
<tr><td>PIW00465</td><td>SY_THR_N_SET_TS_BAND_D</td><td>1</td><td></td></tr>
<tr><td>PIW00466</td><td>SY_THR_N_SET_TS_BAND_C</td><td>1</td><td></td></tr>
<tr><td>PIW00467</td><td>SY_THR_N_SET_TS_BAND_B</td><td>1</td><td></td></tr>
</table>
</td></tr>
</table>

PIW00468	SY_THR_N_SET_TS_BAND_A	1	
PIW01403	SY_THR_N_IS_SEQ_POS	2	
PIW01166	SY_THR_N_SET_IS_FE	PREAMP	
PIW00470	SY_THR_N_SET_IS_TNR2	V1	
PIW00471	SY_THR_N_SET_IS_TNR1	HF_V1_V2	
PIW01403	SY_THR_N_IS_SEQ_POS	6	
PIW01166	SY_THR_N_SET_IS_FE	PREAMP	
PIW00470	SY_THR_N_SET_IS_TNR2	V2	
PIW00471	SY_THR_N_SET_IS_TNR1	HF_V1_V2	
PIW01403	SY_THR_N_IS_SEQ_POS	8	
PIW01166	SY_THR_N_SET_IS_FE	PREAMP	
PIW00470	SY_THR_N_SET_IS_TNR2	V1	
PIW00471	SY_THR_N_SET_IS_TNR1	HF_V1_V2	
PIW01403	SY_THR_N_IS_SEQ_POS	10	
PIW01166	SY_THR_N_SET_IS_FE	PREAMP	
PIW00470	SY_THR_N_SET_IS_TNR2	B_MF	
PIW00471	SY_THR_N_SET_IS_TNR1	HF_V1_V2	
PIW01403	SY_THR_N_IS_SEQ_POS	12	
PIW01166	SY_THR_N_SET_IS_FE	PREAMP	
PIW00470	SY_THR_N_SET_IS_TNR2	V1_V2	
PIW00471	SY_THR_N_SET_IS_TNR1	HF_V1_V2	
PIW01403	SY_THR_N_IS_SEQ_POS	14	
PIW01166	SY_THR_N_SET_IS_FE	PREAMP	
PIW00470	SY_THR_N_SET_IS_TNR2	V2	
PIW00471	SY_THR_N_SET_IS_TNR1	HF_V1_V2	
PIW01403	SY_THR_N_IS_SEQ_POS	16	
PIW01166	SY_THR_N_SET_IS_FE	PREAMP	
PIW00470	SY_THR_N_SET_IS_TNR2	V1_V2	
PIW00471	SY_THR_N_SET_IS_TNR1	HF_V1_V2	
PIW01403	SY_THR_N_IS_SEQ_POS	0	
PIW01166	SY_THR_N_SET_IS_FE	GND	
PIW00470	SY_THR_N_SET_IS_TNR2	V1	
PIW00471	SY_THR_N_SET_IS_TNR1	V1	
PIW01403	SY_THR_N_IS_SEQ_POS	0	
PIW01166	SY_THR_N_SET_IS_FE	PREAMP	
PIW00470	SY_THR_N_SET_IS_TNR2	V1	
PIW00471	SY_THR_N_SET_IS_TNR1	V1	
PIW01403	SY_THR_N_IS_SEQ_POS	0	
PIW01166	SY_THR_N_SET_IS_FE	PREAMP	
PIW00470	SY_THR_N_SET_IS_TNR2	V1	
PIW00471	SY_THR_N_SET_IS_TNR1	V1	
PIW01404	SY_THR_N_HS_SEQ_POS	3	
PIW00473	SY_THR_N_SET_HS_SW	LIST_SWEEP	

PIW00474	SY_THR_N_SET_HS_INIT_FREQ	0	
PIW00475	SY_THR_N_SET_HS_HF2	1	
PIW00476	SY_THR_N_SET_HS_HF1	1	
PIW00477	SY_THR_N_SET_HS_AV	NR_AV_16	
PIW01404	SY_THR_N_HS_SEQ_POS	0	
PIW00473	SY_THR_N_SET_HS_SW	LIST_SWEEP	
PIW00474	SY_THR_N_SET_HS_INIT_FREQ	0	
PIW00475	SY_THR_N_SET_HS_HF2	0	
PIW00476	SY_THR_N_SET_HS_HF1	0	
PIW00477	SY_THR_N_SET_HS_AV	NR_AV_16	
PIW01405	SY_THR_N_HSS_SEQ_POS	4	
PIW00479	SY_THR_N_SET_HSS_S_NR_HF2	160	
PIW00480	SY_THR_N_SET_HSS_S_SIZE_HF2	1	
PIW00481	SY_THR_N_SET_HSS_S_NR_HF1	161	
PIW00482	SY_THR_N_SET_HSS_S_SIZE_HF1	1	
PIW01405	SY_THR_N_HSS_SEQ_POS	0	
PIW00479	SY_THR_N_SET_HSS_S_NR_HF2	0	
PIW00480	SY_THR_N_SET_HSS_S_SIZE_HF2	0	
PIW00481	SY_THR_N_SET_HSS_S_NR_HF1	0	
PIW00482	SY_THR_N_SET_HSS_S_SIZE_HF1	0	
PIW01406	SY_THR_N_DO_AN_SEQ_POS	5	
PIW00484	SY_THR_N_SET_DO_AN_INT	0	
PIW01660	SY_THR_N_SET_DO_AN_MOD	QUIET	
PIW00486	SY_THR_N_SET_DO_AN_EOS	THR_LOOP	
PIW00487	SY_THR_N_SET_DO_AN_CH2	CH2_TNR	
PIW00488	SY_THR_N_SET_DO_AN_CH1	CH1_HFR	
PIW01406	SY_THR_N_DO_AN_SEQ_POS	7	
PIW00484	SY_THR_N_SET_DO_AN_INT	0	
PIW01660	SY_THR_N_SET_DO_AN_MOD	QUIET	
PIW00486	SY_THR_N_SET_DO_AN_EOS	THR_LOOP	
PIW00487	SY_THR_N_SET_DO_AN_CH2	CH2_TNR	
PIW00488	SY_THR_N_SET_DO_AN_CH1	CH1_HFR	
PIW01406	SY_THR_N_DO_AN_SEQ_POS	9	
PIW00484	SY_THR_N_SET_DO_AN_INT	0	
PIW01660	SY_THR_N_SET_DO_AN_MOD	QUIET	
PIW00486	SY_THR_N_SET_DO_AN_EOS	THR_LOOP	
PIW00487	SY_THR_N_SET_DO_AN_CH2	CH2_TNR	
PIW00488	SY_THR_N_SET_DO_AN_CH1	CH1_HFR	
PIW01406	SY_THR_N_DO_AN_SEQ_POS	11	
PIW00484	SY_THR_N_SET_DO_AN_INT	0	
PIW01660	SY_THR_N_SET_DO_AN_MOD	QUIET	
PIW00486	SY_THR_N_SET_DO_AN_EOS	THR_LOOP	
PIW00487	SY_THR_N_SET_DO_AN_CH2	CH2_TNR	

PIW00488	SY_THR_N_SET_DO_AN_CH1	CH1_HFR	
PIW01406	SY_THR_N_DO_AN_SEQ_POS	13	
PIW00484	SY_THR_N_SET_DO_AN_INT	0	
PIW01660	SY_THR_N_SET_DO_AN_MOD	QUIET	
PIW00486	SY_THR_N_SET_DO_AN_EOS	THR_LOOP	
PIW00487	SY_THR_N_SET_DO_AN_CH2	CH2_TNR	
PIW00488	SY_THR_N_SET_DO_AN_CH1	CH1_HFR	
PIW01406	SY_THR_N_DO_AN_SEQ_POS	15	
PIW00484	SY_THR_N_SET_DO_AN_INT	0	
PIW01660	SY_THR_N_SET_DO_AN_MOD	QUIET	
PIW00486	SY_THR_N_SET_DO_AN_EOS	THR_LOOP	
PIW00487	SY_THR_N_SET_DO_AN_CH2	CH2_TNR	
PIW00488	SY_THR_N_SET_DO_AN_CH1	CH1_HFR	
PIW01406	SY_THR_N_DO_AN_SEQ_POS	17	
PIW00484	SY_THR_N_SET_DO_AN_INT	0	
PIW01660	SY_THR_N_SET_DO_AN_MOD	QUIET	
PIW00486	SY_THR_N_SET_DO_AN_EOS	THR_LOOP	
PIW00487	SY_THR_N_SET_DO_AN_CH2	CH2_TNR	
PIW00488	SY_THR_N_SET_DO_AN_CH1	CH1_HFR	
PIW01406	SY_THR_N_DO_AN_SEQ_POS	0	
PIW00484	SY_THR_N_SET_DO_AN_INT	0	
PIW01660	SY_THR_N_SET_DO_AN_MOD	STANDARD	
PIW00486	SY_THR_N_SET_DO_AN_EOS	THR_LOOP	
PIW00487	SY_THR_N_SET_DO_AN_CH2	CH2_TNR	
PIW00488	SY_THR_N_SET_DO_AN_CH1	CH1_TNR	
PIW01406	SY_THR_N_DO_AN_SEQ_POS	0	
PIW00484	SY_THR_N_SET_DO_AN_INT	0	
PIW01660	SY_THR_N_SET_DO_AN_MOD	STANDARD	
PIW00486	SY_THR_N_SET_DO_AN_EOS	THR_LOOP	
PIW00487	SY_THR_N_SET_DO_AN_CH2	CH2_TNR	
PIW00488	SY_THR_N_SET_DO_AN_CH1	CH1_TNR	
PIW01406	SY_THR_N_DO_AN_SEQ_POS	0	
PIW00484	SY_THR_N_SET_DO_AN_INT	0	
PIW01660	SY_THR_N_SET_DO_AN_MOD	STANDARD	
PIW00486	SY_THR_N_SET_DO_AN_EOS	THR_LOOP	
PIW00487	SY_THR_N_SET_DO_AN_CH2	CH2_TNR	
PIW00488	SY_THR_N_SET_DO_AN_CH1	CH1_TNR	
ZIW00115	TC_THR_LOAD_BURST_PAR_1	M	AIWF037K
PIW01407	SY_THR_B_TS_SEQ_POS	1	
PIW00493	SY_THR_B_SET_TS_AV	NR_AV_16	
PIW00494	SY_THR_B_SET_TS_CR	DISABLED	
PIW00495	SY_THR_B_SET_TS_AU	ENABLED	
PIW00496	SY_THR_B_SET_TS_BAND_D	1	

PIW00497	SY_THR_B_SET_TS_BAND_C	1	
PIW00498	SY_THR_B_SET_TS_BAND_B	1	
PIW00499	SY_THR_B_SET_TS_BAND_A	1	
PIW01407	SY_THR_B_TS_SEQ_POS	0	
PIW00493	SY_THR_B_SET_TS_AV	NR_AV_128	
PIW00494	SY_THR_B_SET_TS_CR	DISABLED	
PIW00495	SY_THR_B_SET_TS_AU	DISABLED	
PIW00496	SY_THR_B_SET_TS_BAND_D	1	
PIW00497	SY_THR_B_SET_TS_BAND_C	1	
PIW00498	SY_THR_B_SET_TS_BAND_B	1	
PIW00499	SY_THR_B_SET_TS_BAND_A	1	
PIW01407	SY_THR_B_TS_SEQ_POS	0	
PIW00493	SY_THR_B_SET_TS_AV	NR_AV_128	
PIW00494	SY_THR_B_SET_TS_CR	DISABLED	
PIW00495	SY_THR_B_SET_TS_AU	DISABLED	
PIW00496	SY_THR_B_SET_TS_BAND_D	1	
PIW00497	SY_THR_B_SET_TS_BAND_C	1	
PIW00498	SY_THR_B_SET_TS_BAND_B	1	
PIW00499	SY_THR_B_SET_TS_BAND_A	1	
PIW01407	SY_THR_B_TS_SEQ_POS	0	
PIW00493	SY_THR_B_SET_TS_AV	NR_AV_128	
PIW00494	SY_THR_B_SET_TS_CR	DISABLED	
PIW00495	SY_THR_B_SET_TS_AU	DISABLED	
PIW00496	SY_THR_B_SET_TS_BAND_D	1	
PIW00497	SY_THR_B_SET_TS_BAND_C	1	
PIW00498	SY_THR_B_SET_TS_BAND_B	1	
PIW00499	SY_THR_B_SET_TS_BAND_A	1	
PIW01408	SY_THR_B_IS_SEQ_POS	2	
PIW01167	SY_THR_B_SET_IS_FE	PREAMP	
PIW00501	SY_THR_B_SET_IS_TNR2	V1	
PIW00502	SY_THR_B_SET_IS_TNR1	HF_V1_V2	
PIW01408	SY_THR_B_IS_SEQ_POS	6	
PIW01167	SY_THR_B_SET_IS_FE	PREAMP	
PIW00501	SY_THR_B_SET_IS_TNR2	V2	
PIW00502	SY_THR_B_SET_IS_TNR1	HF_V1_V2	
PIW01408	SY_THR_B_IS_SEQ_POS	8	
PIW01167	SY_THR_B_SET_IS_FE	PREAMP	
PIW00501	SY_THR_B_SET_IS_TNR2	V1	
PIW00502	SY_THR_B_SET_IS_TNR1	HF_V1_V2	
PIW01408	SY_THR_B_IS_SEQ_POS	10	
PIW01167	SY_THR_B_SET_IS_FE	PREAMP	
PIW00501	SY_THR_B_SET_IS_TNR2	B_MF	
PIW00502	SY_THR_B_SET_IS_TNR1	HF_V1_V2	

PIW01408	SY_THR_B_IS_SEQ_POS	12	
PIW01167	SY_THR_B_SET_IS_FE	PREAMP	
PIW00501	SY_THR_B_SET_IS_TNR2	V1_V2	
PIW00502	SY_THR_B_SET_IS_TNR1	HF_V1_V2	
PIW01408	SY_THR_B_IS_SEQ_POS	14	
PIW01167	SY_THR_B_SET_IS_FE	PREAMP	
PIW00501	SY_THR_B_SET_IS_TNR2	V2	
PIW00502	SY_THR_B_SET_IS_TNR1	HF_V1_V2	
PIW01408	SY_THR_B_IS_SEQ_POS	16	
PIW01167	SY_THR_B_SET_IS_FE	PREAMP	
PIW00501	SY_THR_B_SET_IS_TNR2	V1_V2	
PIW00502	SY_THR_B_SET_IS_TNR1	HF_V1_V2	
PIW01408	SY_THR_B_IS_SEQ_POS	0	
PIW01167	SY_THR_B_SET_IS_FE	GND	
PIW00501	SY_THR_B_SET_IS_TNR2	V1	
PIW00502	SY_THR_B_SET_IS_TNR1	V1	
PIW01408	SY_THR_B_IS_SEQ_POS	0	
PIW01167	SY_THR_B_SET_IS_FE	PREAMP	
PIW00501	SY_THR_B_SET_IS_TNR2	V1	
PIW00502	SY_THR_B_SET_IS_TNR1	V1	
PIW01408	SY_THR_B_IS_SEQ_POS	0	
PIW01167	SY_THR_B_SET_IS_FE	PREAMP	
PIW00501	SY_THR_B_SET_IS_TNR2	V1	
PIW00502	SY_THR_B_SET_IS_TNR1	V1	
PIW01409	SY_THR_B_HS_SEQ_POS	3	
PIW00504	SY_THR_B_SET_HS_SW	LIST_SWEEP	
PIW00505	SY_THR_B_SET_HS_INIT_FREQ	0	
PIW00506	SY_THR_B_SET_HS_HF2	1	
PIW00507	SY_THR_B_SET_HS_HF1	1	
PIW00508	SY_THR_B_SET_HS_AV	NR_AV_16	
PIW01409	SY_THR_B_HS_SEQ_POS	0	
PIW00504	SY_THR_B_SET_HS_SW	AUTO_SWEEP	
PIW00505	SY_THR_B_SET_HS_INIT_FREQ	0	
PIW00506	SY_THR_B_SET_HS_HF2	0	
PIW00507	SY_THR_B_SET_HS_HF1	0	
PIW00508	SY_THR_B_SET_HS_AV	NR_AV_16	
PIW01410	SY_THR_B_HSS_SEQ_POS	4	
PIW00510	SY_THR_B_SET_HSS_S_NR_HF2	160	
PIW00511	SY_THR_B_SET_HSS_S_SIZE_HF2	1	
PIW00512	SY_THR_B_SET_HSS_S_NR_HF1	161	
PIW00513	SY_THR_B_SET_HSS_S_SIZE_HF1	1	
PIW01410	SY_THR_B_HSS_SEQ_POS	0	
PIW00510	SY_THR_B_SET_HSS_S_NR_HF2	0	

PIW00511	SY_THR_B_SET_HSS_S_SIZE_HF2	0	
PIW00512	SY_THR_B_SET_HSS_S_NR_HF1	0	
PIW00513	SY_THR_B_SET_HSS_S_SIZE_HF1	0	
PIW01411	SY_THR_B_DO_AN_SEQ_POS	5	
PIW00515	SY_THR_B_SET_DO_AN_INT	0	
PIW01661	SY_THR_B_SET_DO_AN_MOD	QUIET	
PIW00517	SY_THR_B_SET_DO_AN_EOS	THR_LOOP	
PIW00518	SY_THR_B_SET_DO_AN_CH2	CH2_TNR	
PIW00519	SY_THR_B_SET_DO_AN_CH1	CH1_HFR	
PIW01411	SY_THR_B_DO_AN_SEQ_POS	7	
PIW00515	SY_THR_B_SET_DO_AN_INT	0	
PIW01661	SY_THR_B_SET_DO_AN_MOD	QUIET	
PIW00517	SY_THR_B_SET_DO_AN_EOS	THR_LOOP	
PIW00518	SY_THR_B_SET_DO_AN_CH2	CH2_TNR	
PIW00519	SY_THR_B_SET_DO_AN_CH1	CH1_HFR	
PIW01411	SY_THR_B_DO_AN_SEQ_POS	9	
PIW00515	SY_THR_B_SET_DO_AN_INT	0	
PIW01661	SY_THR_B_SET_DO_AN_MOD	QUIET	
PIW00517	SY_THR_B_SET_DO_AN_EOS	THR_LOOP	
PIW00518	SY_THR_B_SET_DO_AN_CH2	CH2_TNR	
PIW00519	SY_THR_B_SET_DO_AN_CH1	CH1_HFR	
PIW01411	SY_THR_B_DO_AN_SEQ_POS	11	
PIW00515	SY_THR_B_SET_DO_AN_INT	0	
PIW01661	SY_THR_B_SET_DO_AN_MOD	QUIET	
PIW00517	SY_THR_B_SET_DO_AN_EOS	THR_LOOP	
PIW00518	SY_THR_B_SET_DO_AN_CH2	CH2_TNR	
PIW00519	SY_THR_B_SET_DO_AN_CH1	CH1_HFR	
PIW01411	SY_THR_B_DO_AN_SEQ_POS	13	
PIW00515	SY_THR_B_SET_DO_AN_INT	0	
PIW01661	SY_THR_B_SET_DO_AN_MOD	QUIET	
PIW00517	SY_THR_B_SET_DO_AN_EOS	THR_LOOP	
PIW00518	SY_THR_B_SET_DO_AN_CH2	CH2_TNR	
PIW00519	SY_THR_B_SET_DO_AN_CH1	CH1_HFR	
PIW01411	SY_THR_B_DO_AN_SEQ_POS	15	
PIW00515	SY_THR_B_SET_DO_AN_INT	0	
PIW01661	SY_THR_B_SET_DO_AN_MOD	QUIET	
PIW00517	SY_THR_B_SET_DO_AN_EOS	THR_LOOP	
PIW00518	SY_THR_B_SET_DO_AN_CH2	CH2_TNR	
PIW00519	SY_THR_B_SET_DO_AN_CH1	CH1_HFR	
PIW01411	SY_THR_B_DO_AN_SEQ_POS	17	
PIW00515	SY_THR_B_SET_DO_AN_INT	0	
PIW01661	SY_THR_B_SET_DO_AN_MOD	QUIET	
PIW00517	SY_THR_B_SET_DO_AN_EOS	THR_LOOP	

PIW00518	SY_THR_B_SET_DO_AN_CH2	CH2_TNR	
PIW00519	SY_THR_B_SET_DO_AN_CH1	CH1_HFR	
PIW01411	SY_THR_B_DO_AN_SEQ_POS	0	
PIW00515	SY_THR_B_SET_DO_AN_INT	0	
PIW01661	SY_THR_B_SET_DO_AN_MOD	QUIET	
PIW00517	SY_THR_B_SET_DO_AN_EOS	THR_LOOP	
PIW00518	SY_THR_B_SET_DO_AN_CH2	CH2_TNR	
PIW00519	SY_THR_B_SET_DO_AN_CH1	CH1_TNR	
PIW01411	SY_THR_B_DO_AN_SEQ_POS	0	
PIW00515	SY_THR_B_SET_DO_AN_INT	0	
PIW01661	SY_THR_B_SET_DO_AN_MOD	QUIET	
PIW00517	SY_THR_B_SET_DO_AN_EOS	THR_LOOP	
PIW00518	SY_THR_B_SET_DO_AN_CH2	CH2_TNR	
PIW00519	SY_THR_B_SET_DO_AN_CH1	CH1_TNR	
PIW01411	SY_THR_B_DO_AN_SEQ_POS	0	
PIW00515	SY_THR_B_SET_DO_AN_INT	0	
PIW01661	SY_THR_B_SET_DO_AN_MOD	QUIET	
PIW00517	SY_THR_B_SET_DO_AN_EOS	THR_LOOP	
PIW00518	SY_THR_B_SET_DO_AN_CH2	CH2_TNR	
PIW00519	SY_THR_B_SET_DO_AN_CH1	CH1_TNR	

Table 7. Configuration applied on-board to mitigate anomaly

7.4 Preamplifier (PA) and deployment mechanism 3D model

Figure below gives the 3D model of the preamplifier (PA) and deployment mechanism used for the three RPW antennas on-board.

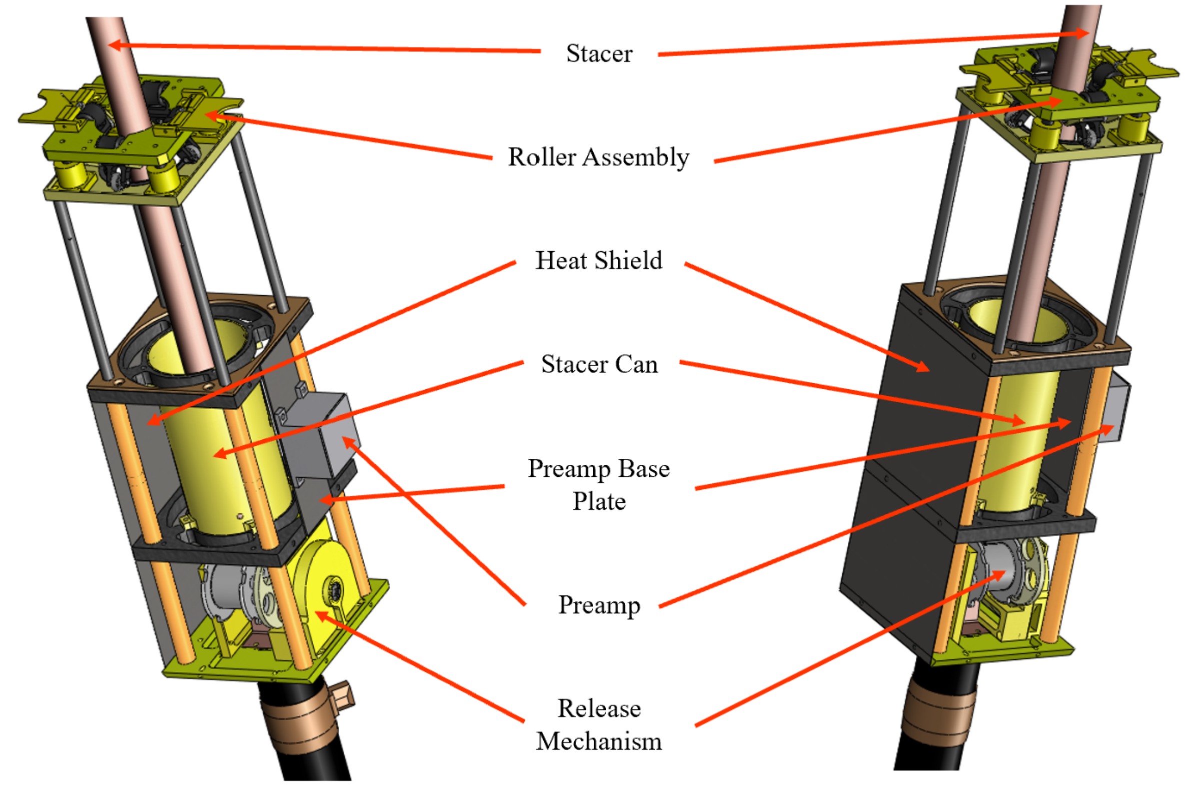

Current SolidWorks Model

Figure 16. RPW antenna preamplifier and deployment mechanim model.

7.5 HF PA with respect to the Bias sweep

It was found that the consumption peaks of the HF preamps are quite linked to the BIAS current sweeps. To understand the cause of these overconsumption peaks and the stress possibly caused on the preamps, a simulation analysis is proposed here.

The analysis is based on a complete model taking into account all stages of the preamp. The output impedance of the BIAS current source is also taken into account (set at 510 kohms). These assumptions are realistic in normal operation of RPW, but are not necessarily representative of the failure case encountered on ANT#3.

7.5.1 Simulation setup

At the HF preamp input, we apply a large ramp of +/-100V to simulate BIAS sweep using a sawtooth waveform. Additionally, the duration of the sweep is arbitrarily chosen to be much smaller than the actual duration of the sweep in flight. This further constrains the simulation results.
Transients caused by such a signal corresponds to an extreme worst case (the sweep used in flight is much more favorable).

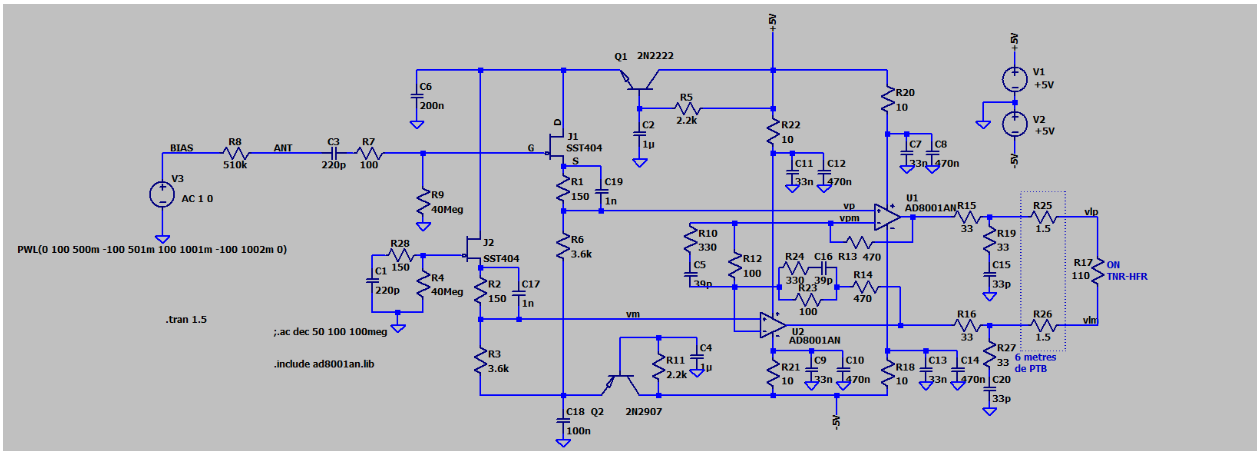

Figure 17. RPW HF PA model used for simulation.

7.5.2 Simulation results

The plots below give the responses of different intermediate signals from the HF preamp, namely:

- VGS, VGD at the JFET stage
- Differential signal at the input of the AD8001
- Ground referenced at the inputs of the AD8001
- Differential signal at the output of the preamp loaded by 110 ohms

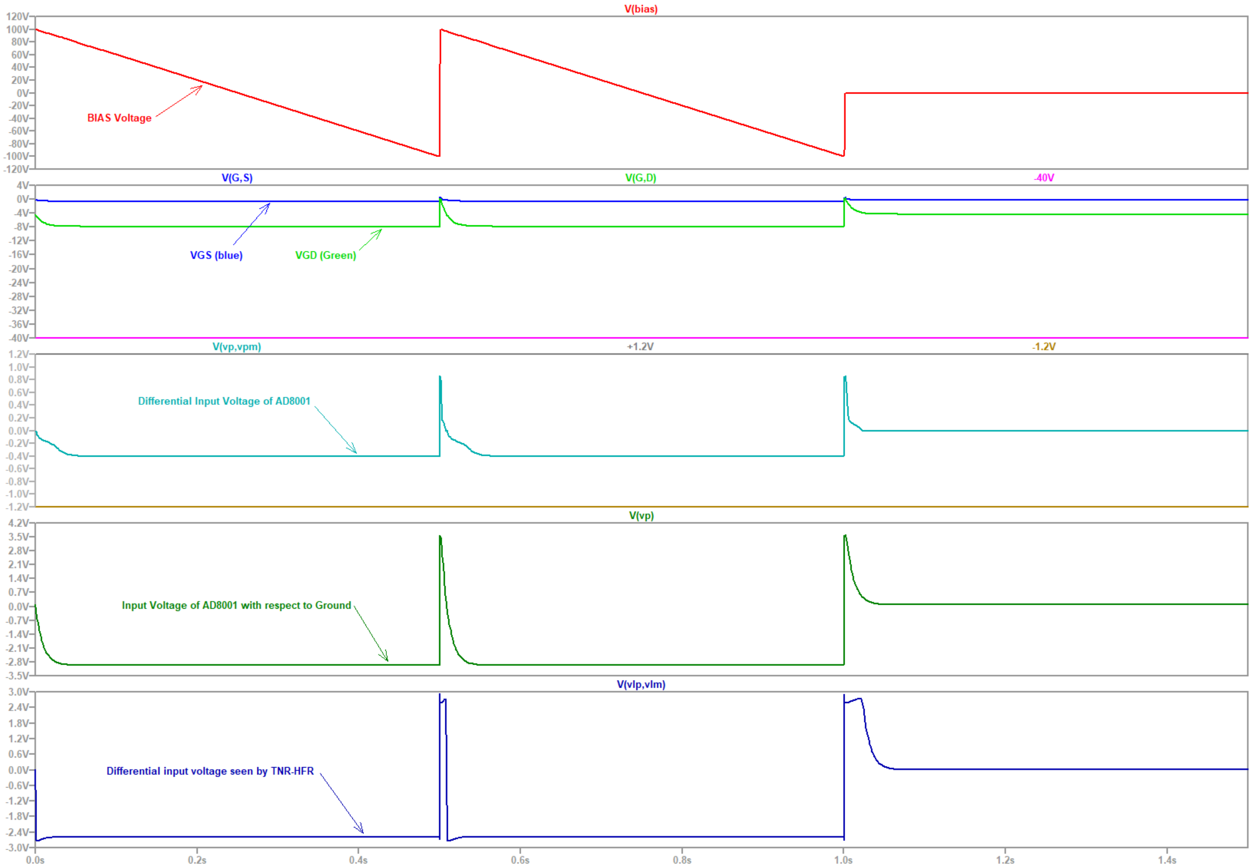

Figure 18. Responses of different intermediate signals from the HF PA.

What arises from these results?

1. The simulation shows that the derating constraints are meet with comfortable margins despite the large ramp of +/-100V
   - VGS is negligible and VGD < -8V; which is far below the -40V limit
   - Differential voltage is comprised between -0.4V and +0.8V, while the limit is +/-1.2V
2. In itself, this observation shows that there is no particular risk in having the BIAS sweep coexist with the HF preamp in operation. It might even be risky to turn it OFF under the pretext of protecting it from BIAS sweeps.
3. The waveform at the output of the preamps (differential signal in blue) shows a relatively narrow and intense pulse. This coincides with the rising edge of the BIAS sweep, which has the effect of saturating the HF preamp for a short duration. This voltage pulse results in excess consumption in the 110 ohms load, which explains the current peaks observed on the monitoring HKs.

This last conclusion, however, has no harmful consequences on HF preamps. After saturation recovery, the HF preamp resumes normal operation without any particular stress.
One possible option to mitigate the problem (which is not necessarily a problem) would be to “smooth” the BIAS sweep : i.e. sweep consisting of an ascending ramp followed by a descending ramp.

7.5.3 About possible latch-up or damages in the HF preamps

A latch-up in an electronic circuit is characterized by a persistent state, which causes overconsumption (observable on the power rails). When it occurs, it usually does not go away on its own. To release it requires an on/off cycle.
This aspect has been carefully taken into account during the design and the latch-up immunity was verified by applying +/-100V short transients to the preamp input. Latch-up never occurs on the second version, which corresponds to the flight one.
In addition, we observed that the HF preamps systematically and almost instantly return to normal consumption after the pulses transients (those caused by the rising edge of the BIAS sweep). This excludes the latch-up hypothesis.
Finally, when the short circuit disappeared and the ANT#3 recovers its function, the observables revealed no difference in behavior before and after the anomaly. If a preamp failure had occurred, it is very likely that its consequences would have been visible in scientific and monitoring data.
A simple failure on the link capacitor (C100) would even have propagated to the LF preamps and would have affected BIAS operation. A double breakdown is very hypothetical and would have been even more visible. However, this is not the case.

7.6 Preliminary observations since ANT3 signal recovery

This section presents the first RPW observations obtained since the return of the ANT3 signal. Analysis of these data is in progress by RPW team.

Figure below presents LFR CWF DC voltage acquired on-board on channel 3 on February 27th, 2024 between 22:40:55z and 22:41:10z. The signal suddently changes from approx. 0.7V to 49V, indicating the V3 monopole signal is not null anymore.

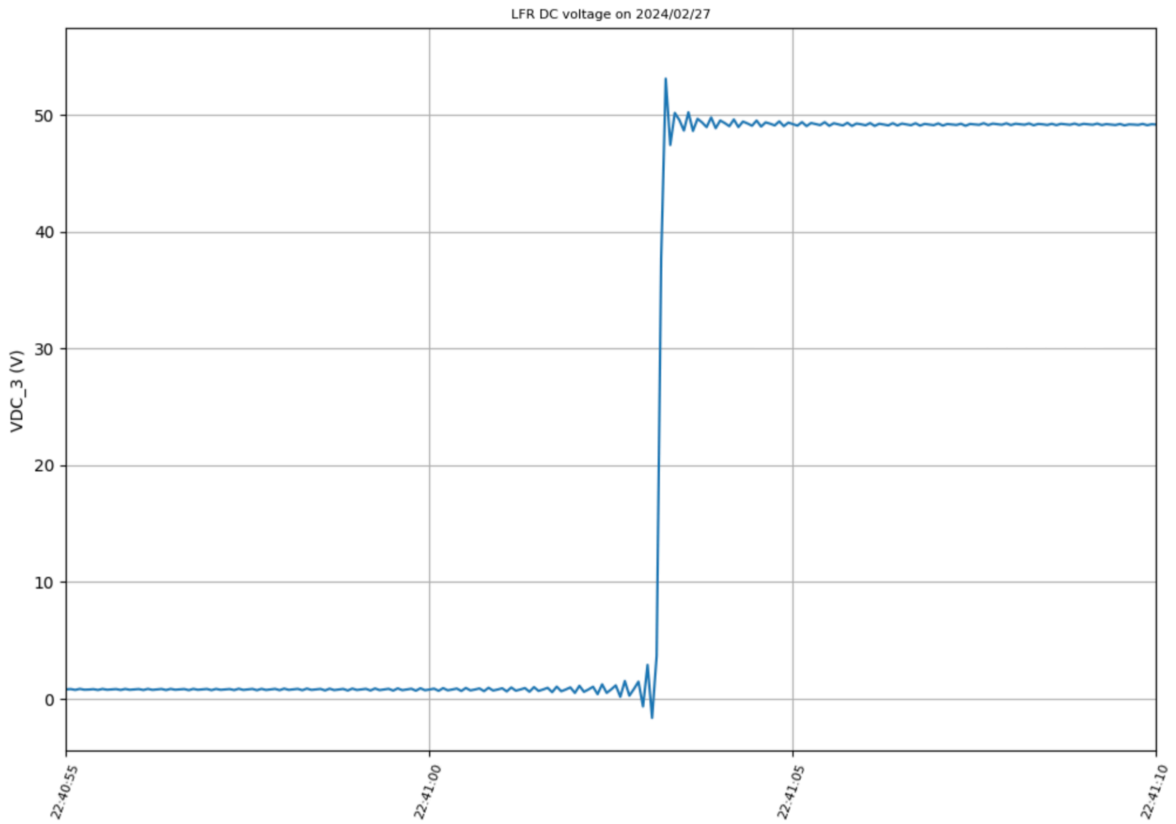

Figure 19. LFR CWF DC voltage measured on Feb. 27, 2024 between 22:40 and 22:41.

This event was also confirmed by TDS. Figures below show TDS E-field spectrograms obtained from TSWF data acquired on-board on February 27th (Figure 20) and 28th (Figure 21) of 2024 respectively. V3 channel (third spectrogram from the top on each figure) shows no signal on Feb. 27, but is come back the next day. On TDS, the time resolution was too low to determinate the time of the event with accuracy.

Bias team has also confirmed that the sweeps on ANT3 have become normal again after this date.

No specific activity concerning RPW or the plateform was scheduled on-board at that time. The reason why ANT3 signal has been recovered is not known at this stage.

Nevertheless ANT3 signal was lost again between ~04:20z and ~20:00z on March 3, 2024, then few hours on March 9, 10, 12 and 14. For the three latter cases, the lost seems to be correlated with Bias sweeps, but it is not the case on March 3. Furthermore, Bias team has reported that there are still intermittent problems with the sweeps (e.g. 12 March 23:28 and 13 March at 23:28). Investigations are still in progress.

Table below summaries the identified periods where ANT3 signal has been temporary lost since Feb. 27, 2024.

Period of ANT3 unavailability	Comments
March 3 between ~04:20z and ~20:00z	Nothing to report
Between March 8 at ~23:38z and March 9 ~04:22z	Bias sweep on ANT3 at start

Between March 9 at ~23:38z and March 10 ~05:59z	Bias sweep on ANT3 at start
Between March 10 at ~23:38z and March 11 ~05:49z	Bias sweep on ANT3 at start
Between March 11 at ~23:38z and March 12 ~01:55z (TBC)	Bias sweep on ANT3 at start
Between March 13 at ~23:38z and March 14 ~04:24z	Bias sweep on ANT3 at start

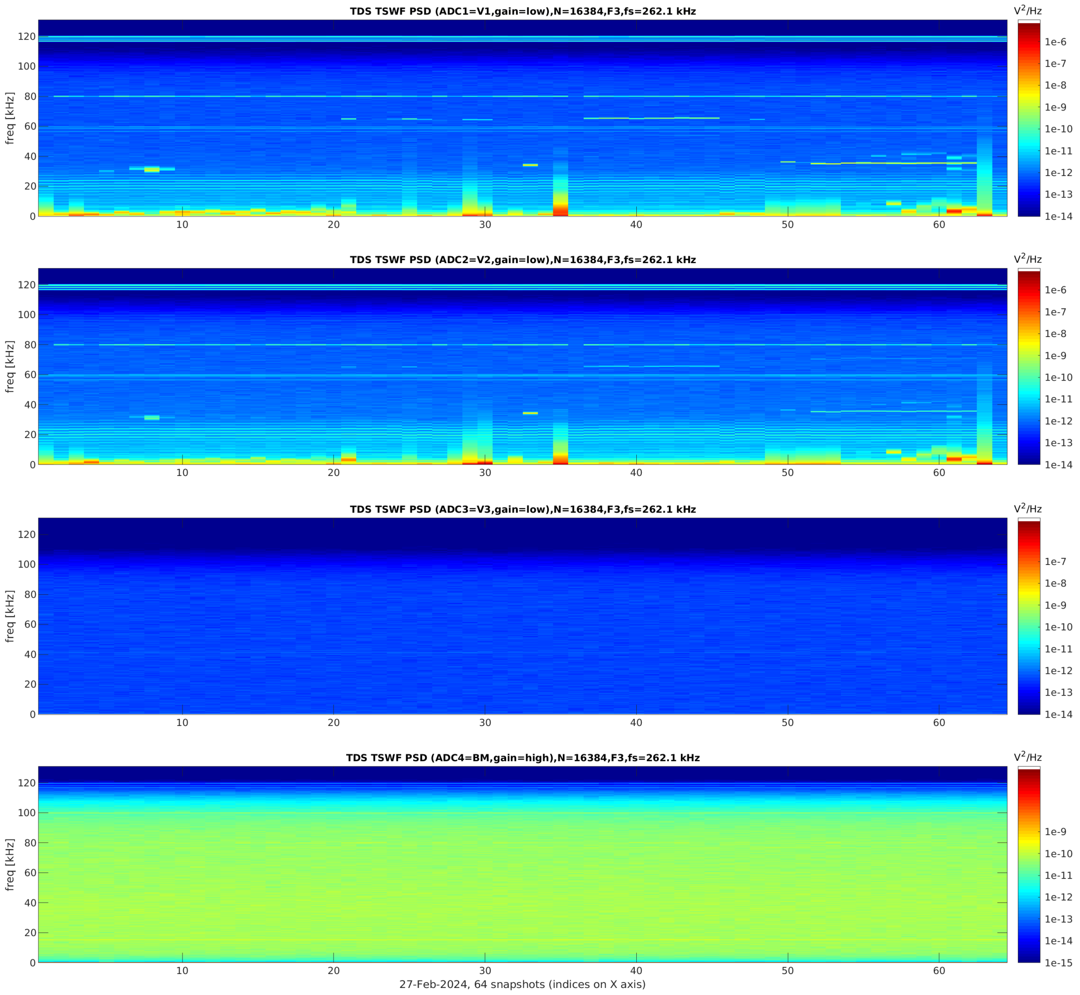

Figure 20. TDS E-field spectrograms from TSWF data acquired on Feb. 27th 2024. V3 channel is the third from the top.

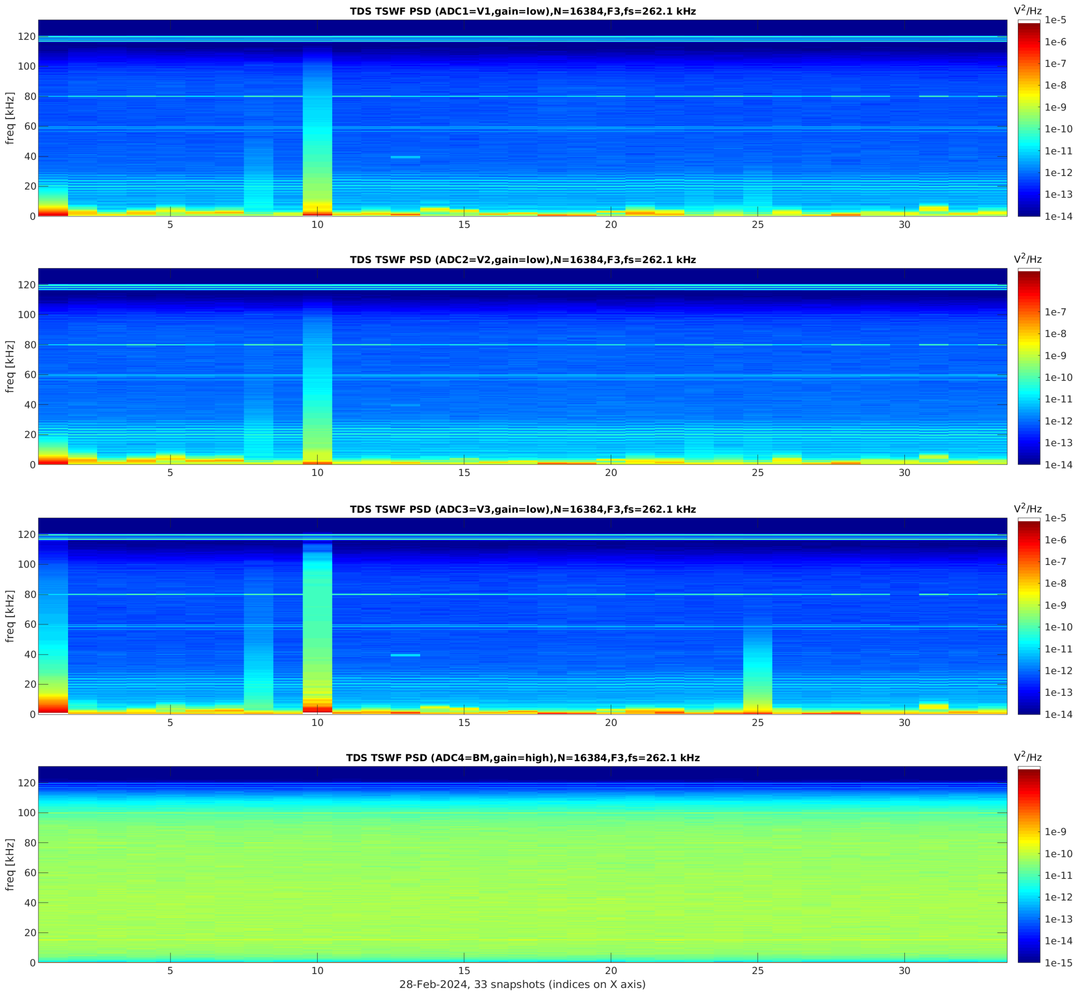

Figure 21. TDS E-field spectrograms from TSWF data acquired on Feb. 28th 2024. V3 channel is the third from the top.

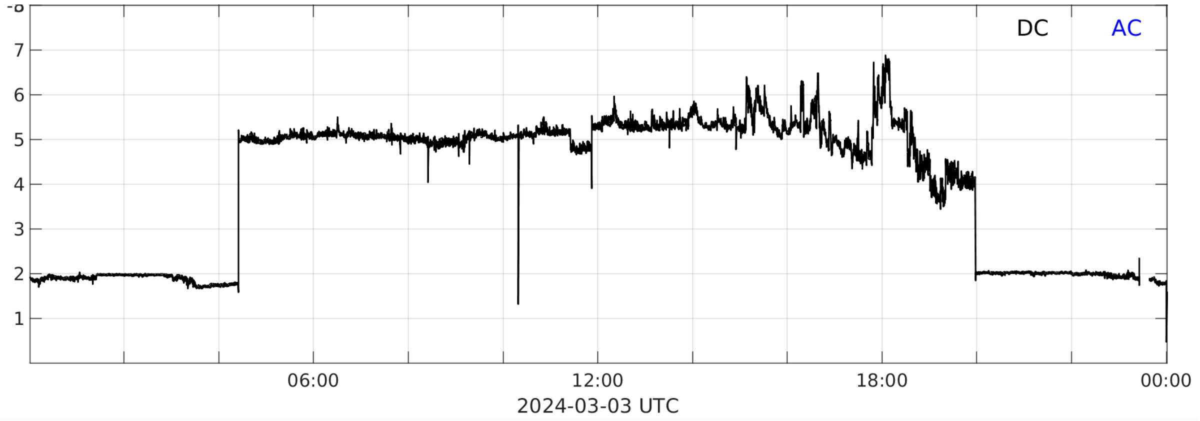

Figure 22. LFR CWF DC field data measured on-board on 2024-03-03.

7.7 Observations from SoloHi ('debris' hypothesis)

Figure below presents a mosaic image from the SoloHI instrument data on Sept. 2024. Image is extracted from a "ratio" movie where background is removed by dividing two consecutive images. Sun is on the right side of the image, hidden by the S/C heatshield. More or less intense black curved lines can be seen close the heatshield (some are indicated by the blue arrows for illustration). These lines, which are often visible in SoloHi data, could be the trace let by heatshield 'debris' (to be confirmed).

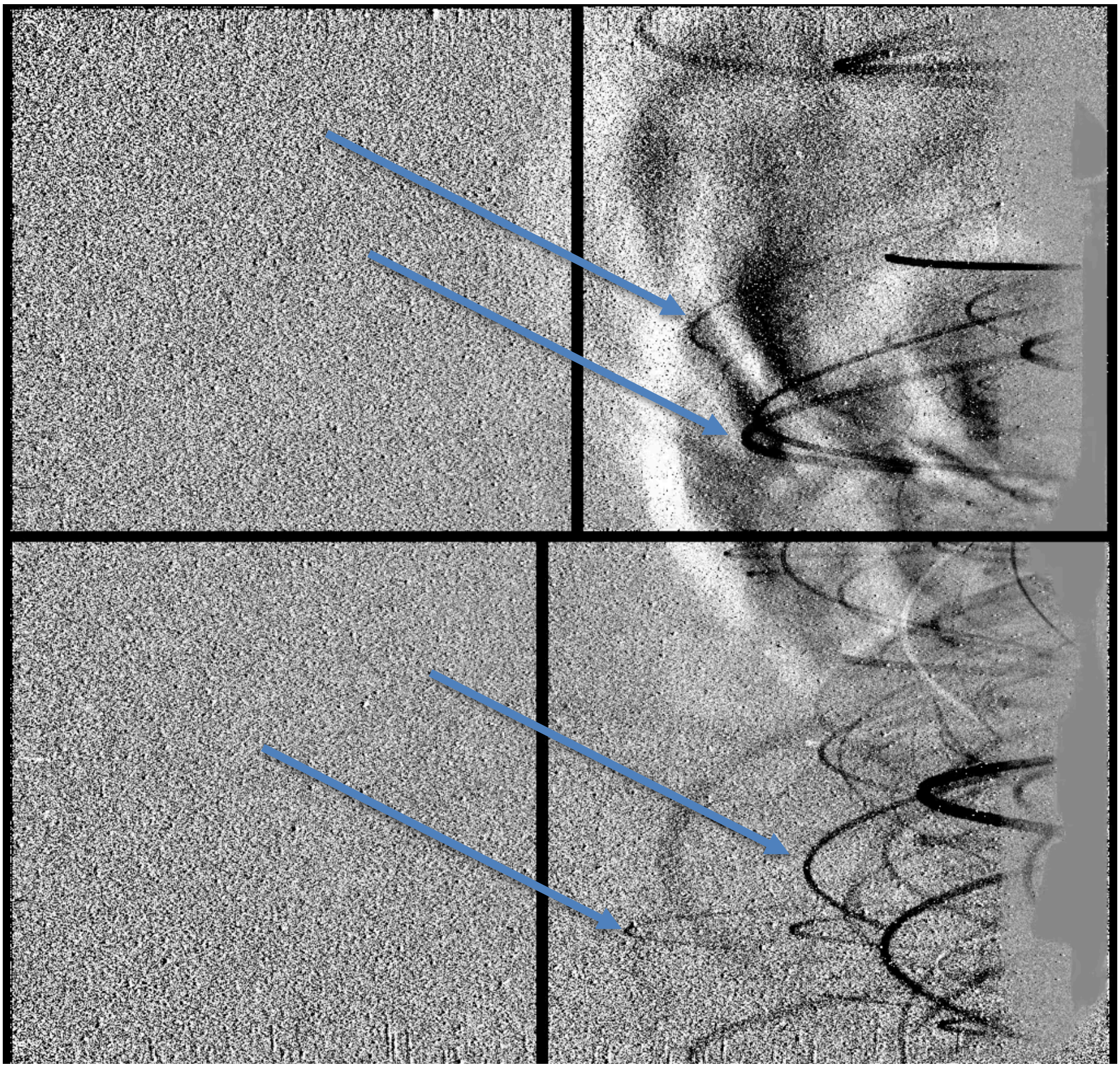

Figure 23. SoloHi mosaic image from Sept. 2023 'ratio' movie

8 LIST OF TBC/TBD/TBWS

TBC/TBD/TBW

Reference/Page/Location	Description	Type	Status